群れとゆらぎの共立

村上，久

(Degree)
博士（理学）

(Date of Degree)
2015-03-25

(Date of Publication)
2017-03-25

(Resource Type)
doctoral thesis

(Report Number)
甲第6333号

(URL)
https://hdl.handle.net/20.500.14094/D1006333

博士論文

群れとゆらぎの共立

平成 27 年 1 月

神戸大学大学院理学研究科
村上　久

Contents

1. Introduction

Collective behavior found in insect swarms, fish schools and mammal herds is a fascinating natural phenomenon [1-5]. Although only local communications are involved, collective animals exhibit rapidly synchronized movements, appearing to behave as if they were part of a single organism [6]. In other words, even though they are a collection of individuals, there is an emergent *collectiveness* as a whole group, such as a *swarm* found in an aggregation of insects. Collective behavior, therefore, is a striking example to consider a living system in the context of the relation between "parts and whole".

Regardless of the kind of species, the similarities in the behavior of different animals suggest that there is a simple rule underlying collective motion. In the study of collective behavior, to understand such the rule, a lot of theoretical models have been proposed. BOID (Bird-andrOID) is a pioneering model that was proposed in computer graphics [7]. An agent in BOID has a neighborhood with fixed radius in which the agent departs from its neighbor if it is too close to the neighbor (collision avoidance), aligns its velocity to those of neighbors by matching the their directions (velocity matching), and approaches to neighbors if it is too far from the neighbors (flock centering). BOID flocks formed from these rules can appear as if it were real to some extent, so that computer animation created with this model has been used in some films.

Most important rule to create collectiveness, however, is considered to be "velocity matching" (VM). The model specialized in VM is so-called SPP (self-propelled particle) [8, 9]. In this model, each agent interacts with neighbors in neighborhood with a fixed radius by averaging the directions of motion of its neighbors (i.e., the velocity matching), coupled with "external noise" with a certain magnitude. On one hand, if there is no external noise, SPPs compose a perfectly aligned group. On the other hand, if there is too much external noise, SPPs create an aggregation of individuals that move randomly. Only with critical-tuned external noise SPP behave naturally. In short, SPP yields an idea that a swarm, herd and flock can be regarded as a critical phenomenon between order state as an entirely aligned group and disorder state as a random aggregation. There is an opposed relationship between velocity matching to create collective group and external noise to collapse the group.

Is there such a conflicted coupling in real animal groups? Unfortunately, it seems not to be. Recent advances in image analysis have made it possible to obtain kinetic data on the movements of real organisms [10-16] and to compare that data with simulation models. These empirical studies reported that there are individuals' movements and changes in the positional relations between neighbors in a coherent group. According to previous models such as SPP, these noisy movements of individuals on the inside of the group appear to collapse the collective motions, but real animal groups realize both coherent collective behavior and individuals' movements. We call such diverse movements of individuals in coherent animal group as "inherent noise".

In the chapter 2, we show individuals' movements of schooling ayu fish as an example of inherent noise. Recent experimental and observational data revealed that the internal structures of collective animal groups are not invariant through time. Rather, individuals can produce noise continuously within their group. These individuals' movements within a group, which appear to collapse the global order and information transfer, can enable interactions with various neighbors. In

this chapter, we show that noise generated inherently in a school of ayus (*Plecoglossus altivelis*) is characterized by various power-law behaviors. First, we show that individual fish move faster than Brownian walkers with respect to the center of the mass of the school as a super-diffusive behavior, as seen in starling flocks. Second, we assess neighbor shuffling by measuring the duration of pair-wise contact and find that this distribution obeys the power law. Finally, we show that an individual's movement in the center of a mass reference frame displays a Lévy walk pattern. Our findings suggest that inherent noise (i.e., movements and changes in the relations between neighbors in a directed group) is dynamically self-organized in both time and space. In particular, Lévy walk in schools can be regarded as a well-balanced movement to facilitate dynamic collective motion and information transfer throughout the group.

In chapter 3, we investigate whether inherent noise can contribute swarming behavior of soldier crabs, conducting an experiment with respect to emergent behavior. Emergent behavior that arises from a mass effect is one of the most striking aspects of collective animal groups. Investigating such behavior would be important in order to understand how individuals interact with their neighbors. Although there are many experiments that have used collective animals to investigate social learning or conflict between individuals and society such as that between a fish and a school, reports on mass effects are rare. In this study, we show that a swarm of soldier crabs could spontaneously enter a water pool, which are avoided by a solitary individual, by forming densely populated part of a swarm at the edge of the water pool. Moreover, we show that the observed behavior can be explained by the model of collective behavior based on inherent noise that is individuals' different velocities in a directed group. Our results suggest that inherent noise, which is widely seen in collective animals, can contribute to formation and/or maintenance of a swarm and that the dense swarm can enter the pool by means of enhanced inherent noise.

In chapter 4, we explain animal foraging strategy by our new foraging model, as an introduction for collective animal foraging that will be shown in the chapter 5. In intermittent random search in which slow motion to detect the target is discretely separated from the motion to migrate to another feeder, the high efficiency of Lévy strategy, i.e. time interval to switch these two phases is chosen from Lévy distribution, is generally found. While it is reported that Lévy strategy is consistent with searching behavior of real animals, some researchers claim that Levy-like distribution shown by animals is not necessarily produced by Levy process. We here propose an intermittent search model consisting of two phases that is not incorporated with Lévy process. In this model, agent is basically correlated random walker (CRW), but memorizes its trajectory and counts the number of crossover in a trajectory. If the number exceeds a threshold, the agent resets the memory of trajectories and makes ballistic movement in the direction uncorrelated to the past. We also show that this model can balance a trade-off between macro search (exploration) and micro one (exploitation), which is shown by CRW. Finally we demonstrate that another intermittent search model that is incorporated with ambiguity with respect to the rule to switch two phases, can show Lévy-like distribution of the time interval.

In chapter 5, we investigate whether collective animal foraging behavior is driven by inherent noise or not. We here conducted an experiment with respect to collective foraging behavior of a swarm of soldier crabs *Mictyris guinotae*, which live in the tideland and can form large swarms. By using markers

attached to crabs' shells and image-processing software, we obtained time series of individuals' position during thirty minutes. To investigate the behavior, we created two experimental apparatus: ring- and round-shaped arenas. First, we checked basic behavior of soldier crab swarm in the round-shaped arena. Next, to examine characteristics of the behavior, and to simplify analysis, we used the ring-shaped arena. In the ring-shaped arena, the behavior of crabs would be regarded to be approximately one-dimensional. We here investigated whether soldier crabs formed denser swarm on the inside of the arena, and whether they showed collective foraging behavior.

Finally, we summarize the thesis in the conclusion.

2. Inherent Noise can Appear as Several Power-law Behaviors in Fish School

2.1. Background

Although only local interactions are involved, collective animals (e.g., bird flocks and fish schools) exhibit rapidly synchronized movements, appearing to behave as if they were part of a single organism [6]. Information transfer through the entire group when it is exposed to predation is one of the most intriguing aspects of collective animal groups and has been observed, for example, as the propagation of a density wave within a group [17]. In theoretical studies, numerous simulation models have been proposed to understand the spontaneous emergence of the global order and information transfer in a group based on inter-individual interaction in a bottom-up manner [18-22]. In most models, the explicit alignment rule, according to which an agent matches its velocity with others in its neighborhood, is assumed, although the latest empirical research suggests that there is no evidence of direct matching of velocity and that global polarization results from interactions other than those that follow the explicit alignment rule [23].

It is clear, however, that information transfer is propagated by local interactions. Such information transfer can occur even if an individual does not change its relative position with respect to its neighbors, as with magnetic spin, but real animals in a collective group can change its relative position with their neighbors [24]. These individuals' movements on the inside of the group, which appear to collapse the global order and information transfer, can enable interactions with various neighbors and contribute to dynamic collective behavior.

Indeed, recent advances in image analysis have revealed that the internal structures of collective animal groups, in particular flocks and schools, are not fixed in time [15,16,25]. On one hand, when looking at an instant in time, individuals in a group can appear to be highly polarized and directed. Moreover, even velocity fluctuations of different individuals are correlated with each other [16]. On the other hand, in the long term, it has been observed that there is a noise generated inherently in collective animal groups, i.e., individuals travel in a directed group and perpetually replace their position with neighbors. Cavagna and others [24] investigated individual motions on the inside of starling flocks by identifying individual birds' coordinates temporally and observing them in the center of a mass reference frame. In the center of a mass reference frame, one can obtain individuals' coordinates with respect to the center of gravity and, hence, their relative movements with respect to the center of gravity. In their empirical research, Cavagna and colleagues estimated how much a bird moved within the group by calculating the mean-square displacement. They found that the mean-square displacement as a function against time was well described by a power-law dependence and that birds showed supper-diffusive behavior, i.e., they moved faster than Brownian walkers with respect to the center of the mass of the flock. Moreover, the researchers revealed that the remaining rate of a certain number of nearest neighbors exponentially decayed with time. In other words, the birds perpetually reshuffled their

neighbors.

In this study, we investigate individuals' movements on the inside of their group under controlled laboratory conditions using juvenile ayu schools (*Plecoglossus altivelis*) with 10, 20, 30, 40, 50 and 60 individuals. By using video cameras with high temporal resolution (120 frames per second) and image processing software, we obtain identified individuals' trajectories. Then, we investigate diffusion properties and find that ayu fish also move faster than Brownian walkers with respect to the center of the mass of the school, as seen in starling flocks. Next, we assess neighbors' shuffling by measuring pair-wise contact duration and find that there is no characteristic time scale in which individuals remain neighbors. We show that the individuals' movements within the group reveal a Lévy walk pattern with a power-law distribution of step length. Finally, we discuss whether inherent noise in the group [26,27] appearing as Lévy walk is well-balanced movement to facilitate dynamic collective motion and information transfer over the whole group rather than merely erroneous random motions derived from velocity matching among individuals.

2.2. Materials and Methods

2.2.1. Experimental Setup

We studied ayu *Plecoglossus altivelis,* also known as sweetfish, which live throughout Japan and are farmed widely in Japan. Juvenile ayus (approximately 7-14 cm in body length) display typical schooling behavior, though adult ayus tend to show territorial behavior in environments where fish density is low [59]. We purchased juveniles from Tarumiyoushoku (Kasumigaura, Ibaraki, Japan) and housed them in a controlled laboratory. Approximately 150 fish lived in a 0.8 m^3 tank with continuously filtered and recycled fresh water with a temperature maintained at 16.4 °C, and were fed commercial food pellets. Immediately before each experiment was conducted, randomly chosen fish were separated into each school size and moved to an experimental arena without pre-training.

The experimental arena consisted of a 3 × 3 m white shallow tank. The water depth was approximately 8 cm so that schools would be approximately 2D. The fish were recorded with an overhead gray-scale video camera (Library GE 60; Library Co. Ltd., Tokyo, Japan) at a spatial resolution of 640 × 480 pixels and a temporal resolution of 120 frames per second. Schooling fish exhibit two typical ordered states. The first is a polarized state in which they exhibit a turning movement and in which individuals tend to be highly polarized through the group, and the second is a milling state in which individuals exhibit high polarization locally but the group conducts a rotating movement as a whole. In the school of ayus, both of these states were observed. The polarized and milling patterns can be distinguished by using two order parameters [29]—a polarization parameter $O_P=(1/N)|\Sigma^N_{i=1} u_i|$ and a rotation parameter $O_R=(1/N)|\ \Sigma^N_{i=1} u_i \times q_i|$—where u_i is the unit direction of fish number i and q_i is the unit vector pointing from the school's center of mass toward fish i. Each order parameter takes values of between 0 (no alignment or rotation) and 1 (strong alignment or rotation). Hence, we defined polarized patterns as those with high values of the polarization parameter and low values of the rotation parameter and milling patterns as those with high values of the rotation parameter and low values of the polarization parameter. In this study, we used 6 schools—with 10, 20, 30, 40, 50

and 60 individuals—for the polarization pattern and one school, with 40 individuals, for the milling pattern for a total of 7 schools (table 1). All experimental procedures were approved by the University of Tsukuba Animal Use and Care Committee.

2.2.2. Tracking

Time series of identified individuals' positions were tracked using image-processing software (Library Move-tr/2D ver. 8.31; Library Co. Ltd., Tokyo, Japan) on gray-scale images. The shape of each fish and its geometric center were identified by the fact that the fish appear darker than the surrounding area, and the fish trajectories were constructed by tracking individuals from one frame to the next. When fish overlapped or made contact with others, we separated them using the manual tracking mode of the software. As a result, for each observed time duration T, we obtained all of the individuals' x–y coordinates as a single pixel with a side length of 4.76 mm (table 1). In this study, the time interval between two consecutive reconstructions of individuals' coordinates was dt=0.1 sec (12 frames).

Number of individuals	**State of school**	**School size (mm)**	**Total time interval (sec)**	O_p	O_r
10	polarized	414.6	141.5	0.869	0.111
20	polarized	720.16	41.6	0.823	0.183
30	polarized	1232.0	36.0	0.858	0.147
40	polarized	1560.3	19.1	0.799	0.106
50	polarized	1513.4	16.7	0.800	0.263
60	polarized	1557.1	10.0	0.905	0.212
40	milling	1557.7	52.1	0.139	0.849

Table 1. Data of analyzed schools. School size is defined as the maximum distance between two fish belonging to the school O_p and O_r indicate the order parameters for polarization and rotation, respectively. The state of the school is considered as polarized at a high value of O_p and a low value of O_r and as milling at a high value of O_r and a low of O_p. See also in the main text.

2.3. Results

2.3.1. Diffusion in the Fish School

We first investigated diffusive behavior in the polarized schools, a behavior that has been observed in starling flocks [24]. The center of the mass reference frame is useful for observations of

individuals' movements on the inside of their group. To quantify how much individuals move on the inside of their group, one can use the mean-square displacement in the center of the mass reference frame as a function of time (i.e., at the average amount of distance travelled in a time t):

$$\delta r^2(t) = \frac{1}{T-t}\frac{1}{N}\sum_{t_0=0}^{T-t-1}\sum_{i=1}^{N}[r_i(t_0+t)-r_i(t_0)]^2 \quad (1)$$

where $R_i(t)$ indicates the position of i at time t, $R_{CM}(t)$ indicates the position of the center of the mass of the school at time t, and $r_i(t)=R_i(t)-R_{CM}(t)$ therefore represents the position of fish i in the center of the mass reference frame. We averaged over all N fish and over all time lags of duration t in the interval [0, T], where T is the total time interval. In figure 1, we show some trajectories of the school in the camera's reference frame and in the center of the mass reference frame. We estimated $\delta r^2(t)$ with 1.5 orders of magnitude for time (this value is longer than the duration observed in starling flocks [24]), i.e., from 0.1 to 3.2 seconds (see figure 2). This approach was taken because although we can estimate how much individuals move by calculating the mean-square displacement in the center of the mass reference frame, the area where fish can move is, of course, restricted in the interior of school.

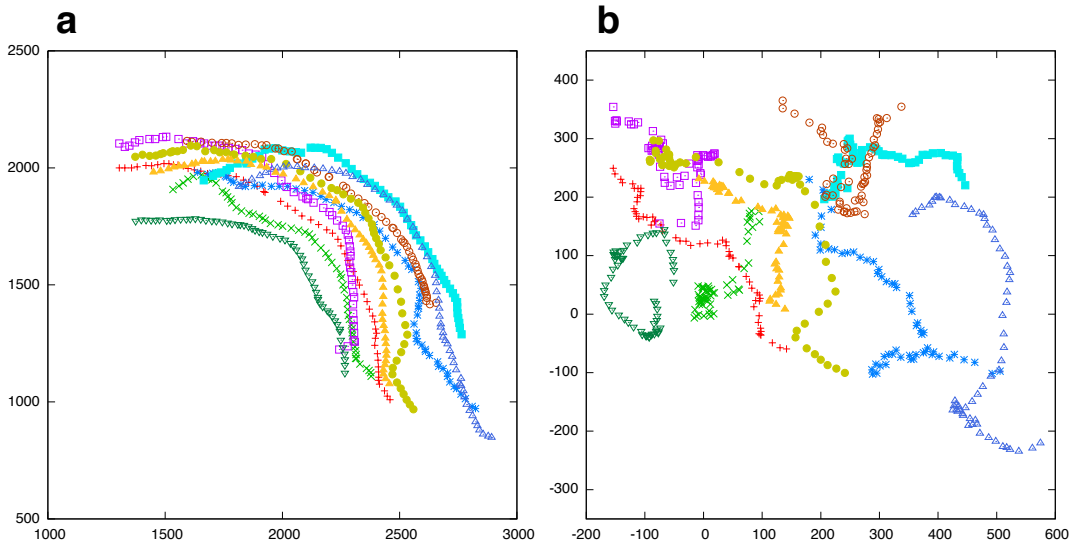

Figure 1. 2D reconstruction of some trajectories of a school. (a) Laboratory reference frame. (b) Center of mass reference frame. All the axes are in millimeters.

By computing $\delta r^2(t)$ for schools, we observed that the mean-square displacement in the center of the mass reference was well-described by the following power-law equation:

$$\delta r^2(t)=Dt^{\alpha} \quad (2)$$

where α is the diffusion exponent, falling between 0 and 2, and D is the diffusion coefficient. Brownian

random walkers diffuse with α=1, corresponding to normal diffusion [44,60]. If α>1, walkers or particles show faster diffusion, which is called super-diffusion. If α=2, particles show ballistic diffusion. We found that the diffusion of fish in each school size fits the equation (2) well, with each exponent being larger than 1 (10 individuals: α=1.34, D=0.0054; N=32, R^2=0.99, F=41.2, $P<10^{-18}$; 20 individuals: α=1.52, D=0.0099; N=32, R^2=0.99, F=186.2, $P<10^{-28}$; 30 individuals: α=1.57, D=0.013; N=32, R^2=0.99, F=700.7, $P<10^{-36}$; 40 individuals: α=1.63, D=0.017; N=32, R^2=0.99, F=3315.7, $P<10^{-47}$; 50 individuals: α=1.75, D=0.012; N=32, R^2=0.99, F=1084.9, $P<10^{-39}$; 60 individuals: α=1.73, D=0.016; N=32, R^2=0.99, F=24543.3, $P<10^{-60}$). Hence, fish display super-diffusive behavior in the center of the mass reference frame. Figure 2 shows the mean-square displacement in the center of the mass reference frame against time for four schools.

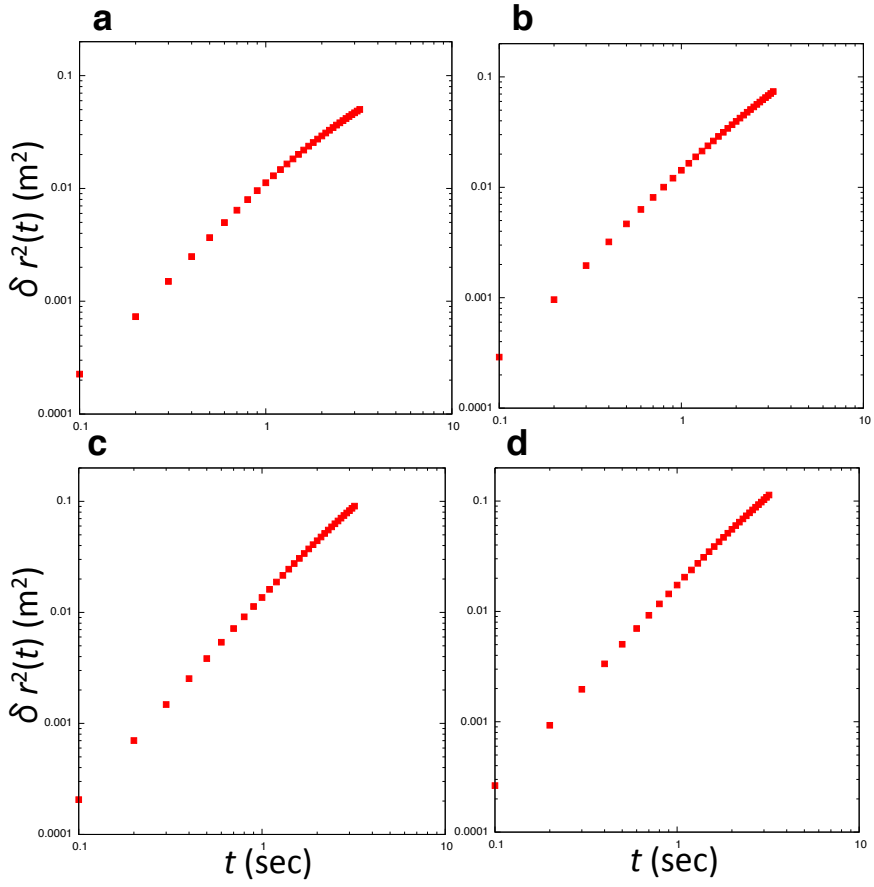

Figure 2. Mean-square displacement in the center of the mass reference frame for four schools. (a) 20 individuals. (b) 30 individuals. (c) 50 individuals. (d) 60 individuals.

2.3.2. Contact Duration as an Estimation of Neighbor Shuffling

Next, we investigated neighbor shuffling in schools. Cavagna and colleagues [24] assessed neighbor changing in bird flocks by calculating the proportion of birds that remained as one of a number of nearest neighbors of focal birds, indicating that neighbor changing declined exponentially against

time. The authors concluded that neighbor reshuffling does occur and that there was no indication of a preferred structure of neighbors in the flock. Instead of computing such proportions, in this study, we estimate neighbor shuffling by investigating contact duration time.

Recently, by using mobile devices that can assess mutual proximity in a distributed manner, person-to-person interactions in various human communities (e.g., offices, hospitals, conferences and so on) have been analyzed systematically [61-63]. In such empirical research, it has been revealed that the contact duration time of pairs within a 1-2 m detection range exhibited a power-law distribution. Because this type of analysis indicates how long individuals interact with their neighbors, we can apply it to fish schools to quantify neighbor shuffling using individuals' temporal coordinates. When we define two fish as a pair if they are within the detection range r_d=60 (mm), we find that the contact duration of pairs of fish shows a power-law distribution in each polarized school (power-law vs. exponential [49]; 10 individuals: N=690, the scaling exponent μ_c=−1.96, AIC weights of power-law $w(p)$=1.00; 20 individuals: N=383, μ_c=−1.92, $w(p)$=1.00, 30 individuals: N=221, μ_c=−2.10, $w(p)$=1.00, 40 individuals: N=137, μ_c=−1.91, $w(p)$=1.00, 50 individuals: N=231, μ_c=−1.89, $w(p)$=1.00, 60 individuals: N=127, μ_c=−1.94, $w(p)$=1.00). Interestingly, the power-law distribution is also found in the milling school (40 individuals: N=171, μ_c=−1.89, $w(p)$=0.95). These results indicate that neighbor shuffling estimated by contact duration in both the polarized and milling schools has a similar structure in time, which agrees with results observed in human communities. Figure 3 shows the cumulative distribution of the contact duration of three polarized schools and one milling school.

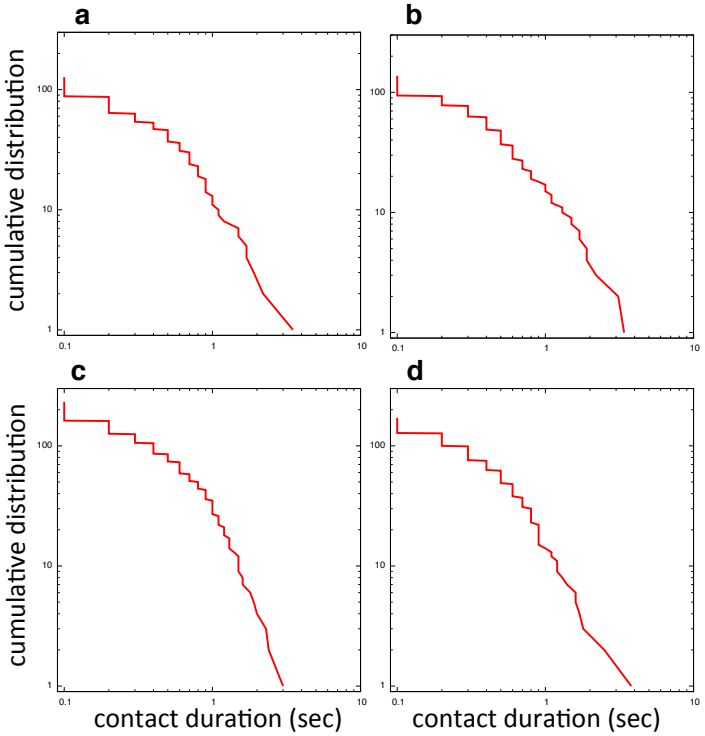

Figure 3. Cumulative distributions of contact duration for four schools. (a) Polarized school with 30 individuals. (b) Polarized school with 40 individuals. (c) Polarized school with 50 individuals. (d) Milling school with 40 individuals.

2.3.3. Lévy Walk in Fish Schools

The super-diffusive movement described above is one of the characteristics of the Lévy walk [44]. The Lévy walk describes a pattern composed of small-step clusters separated by longer relocations [52], in which the distribution of step-length l is as follows:

$$P(l) \sim l^{\mu} \quad \text{with } 1<\mu\leq 3, \tag{3}$$

where μ represents the power-law exponent. Here, we show that fish behave as Lévy walkers on the inside of schools.

The step length can be defined in different ways, such as the distance between consecutive landings on the sea surface for albatross [44,50] and the saccade interval length for fruit flies [64]. To investigate whether the fish log-scale movement lengths in the schools followed power-law distributions, we define the step-length as the intermittent interval length [65] in the trajectories in the center of the mass reference frame as follows: If $dr<|r_i(t)-r_i(t-dt)|$, i.e., if the distance between consecutive positions of i in the center of the mass reference are closer than dr, $r_i(t)$ is considered to be a pausing point. Here, we set dr=20(mm). When we calculate turning angle per dt at both pausing and non-pausing points for all polarized schools (figure 4A), we find that turning angle at pausing points is significantly larger than that at non-pausing points (T-test; pausing points (N = 4156, Mean ± SD = 46.91 ± 45.79 (degree)) vs non-pausing points (N = 3341, Mean ± SD = 17.63 ± 22.82 (degree)); $p<10^{-232}$, T-value=76.18) (figure 4B), where non-pausing point is defined as a position that is not pausing point and whose one next and one before positions are also not pausing point.

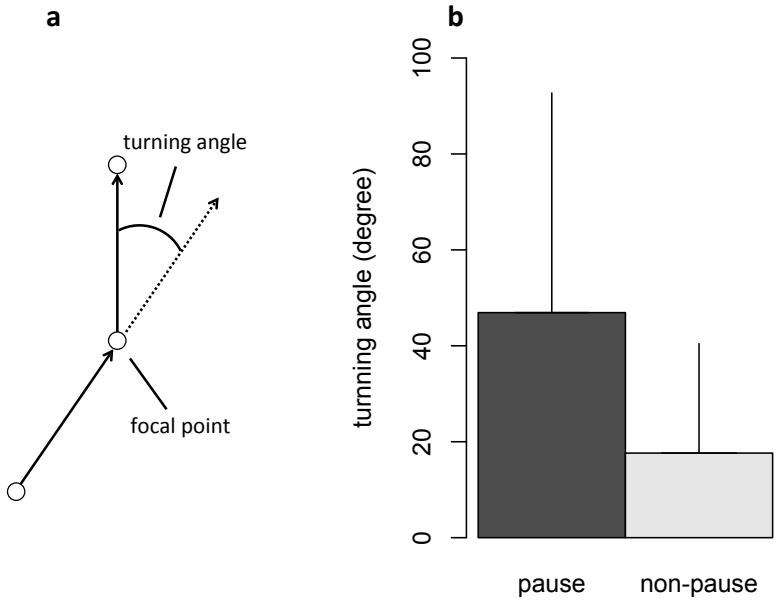

Figure 4. Turning angle at pausing points and non-pausing points. (a) Schematic diagram of turning angle. (b) Mean turning angle at pausing points (dark grey) and non-pausing points (pale grey). Error bars are SDs.

The step-length l ($>dr$) is then considered as the distance between any two successive pausing points. We find that the step lengths of each polarized school follow a power-law distribution (power law vs. exponential; 10 individuals: N=1171, μ=2.97, $w(p)$=1.00; 20 individuals: N=621, μ=2.49, $w(p)$=1.00, 30 individuals: N=769, μ=2.11, $w(p)$=1.00, 40 individuals: N=624, μ=2.18, $w(p)$=1.00, 50 individuals: N=546, μ=2.53, $w(p)$=1.00, 60 individuals: N=489, μ=2.43, $w(p)$=1.00). Because each exponent μ systematically ranges in the interval $1<\mu\leq3$, these results indicate that fish behave as Lévy walkers on the inside of schools. Moreover, when we check an individual's trajectory, its step lengths also show a power-law distribution (power law vs. exponential; one individual: N=102, μ=2.78, $w(p)$=1.00) (for more data of each fish belonging to schools with 10, 20 and 30 individuals see section 2.3.4). Figure 5 shows the cumulative distributions of the step lengths of three polarized schools and of an individual.

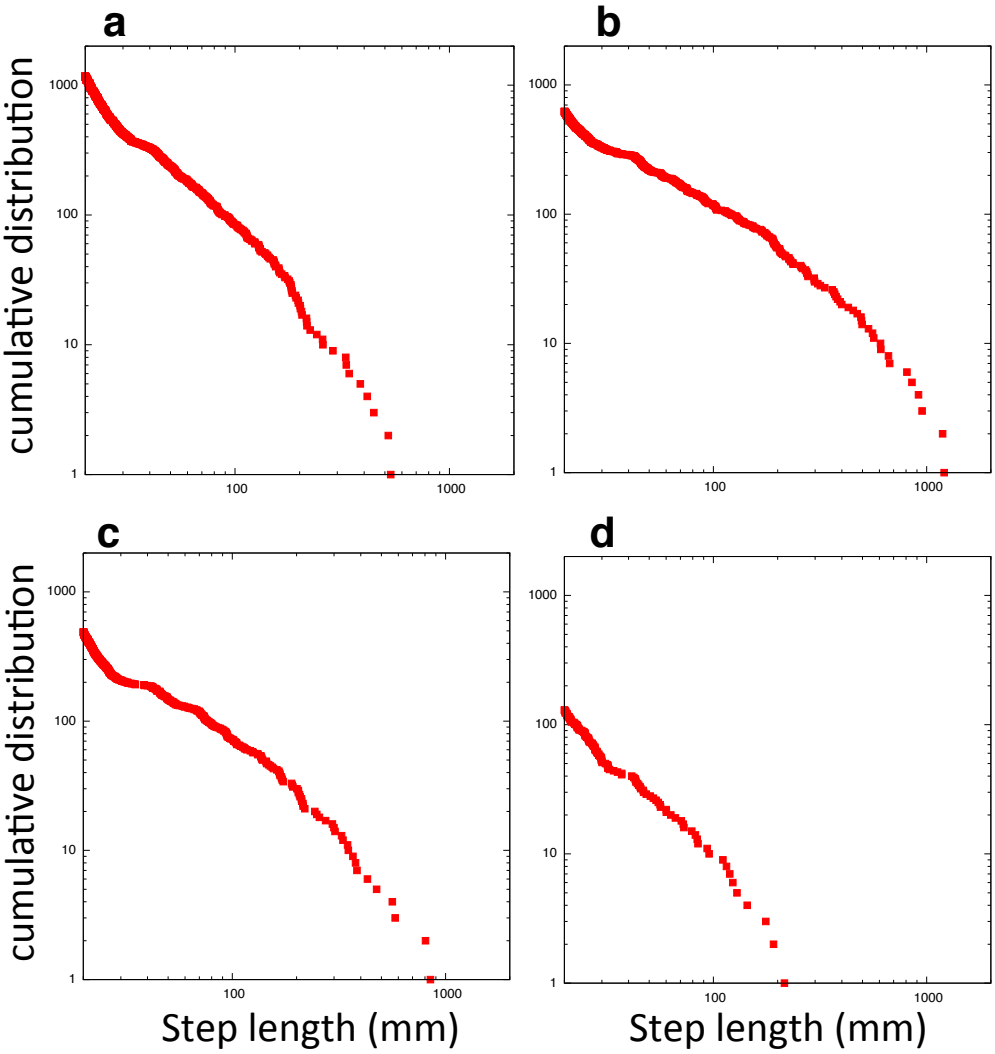

Figure 5. Cumulative distributions of step length in the center of the mass reference frame. (a) 10 individuals. (b) 40 individuals. (c) 60 individuals. (d) One individual.

In figure 6, we present a longer trajectory of an individual in the center of the mass reference frame (for four more samples see section 2.3.4). It is easy to see that there are step clusters separated by longer relocations, which is a characteristic of the trajectory described by a Lévy walk.

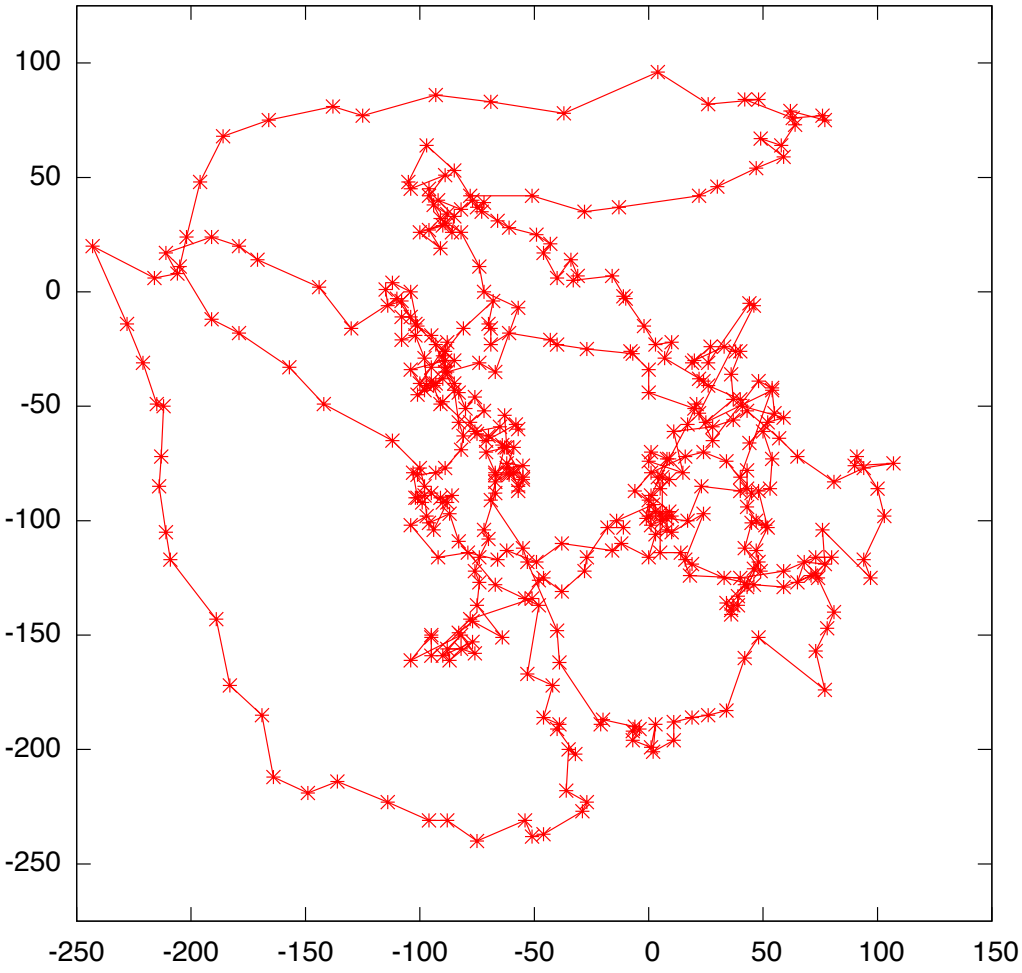

Figure 6. Longer trajectories of an individual in the center of the reference frame. The axes are in millimeters.

2.3.4. Additional Data of Lévy Walk Shown by Individual Fish

In this section, we supply more data of each fish belonging to schools with 10, 20 and 30 individuals with respect to Lévy walk in schools, and four more samples of longer trajectory of an individual in the center of the mass reference frame.

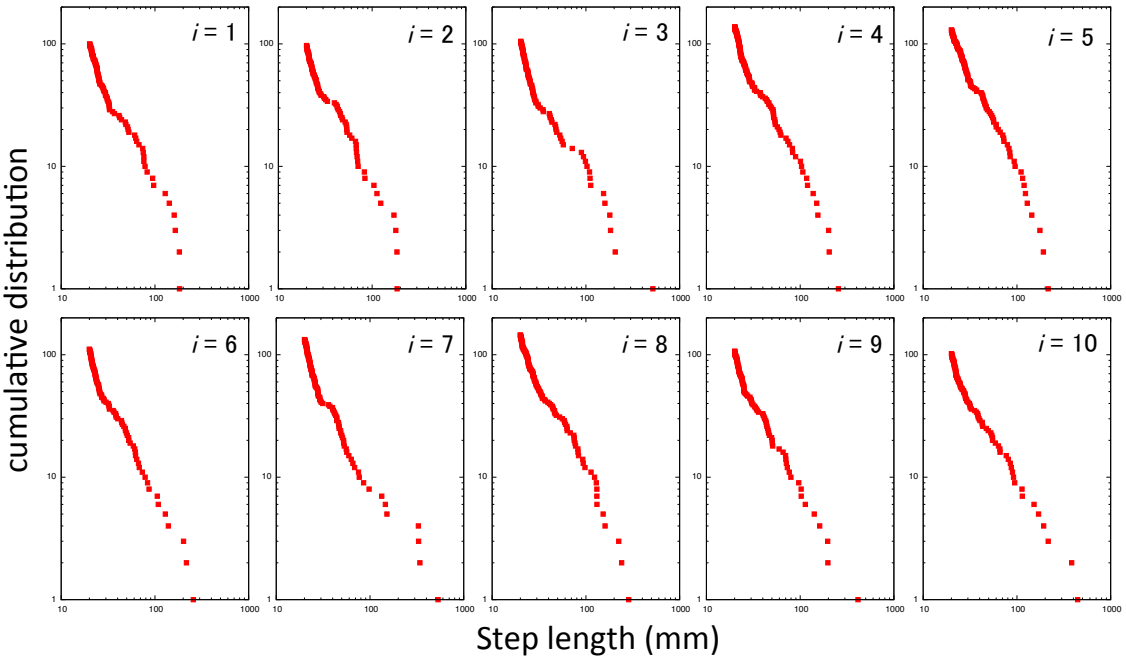

Figure 7. Cumulative distributions of step-lengths in the center of mass reference frame, displayed by each individual fish belonging to 10 individuals school. Number *i* in each plot indicates individual number that corresponds as in table 2.

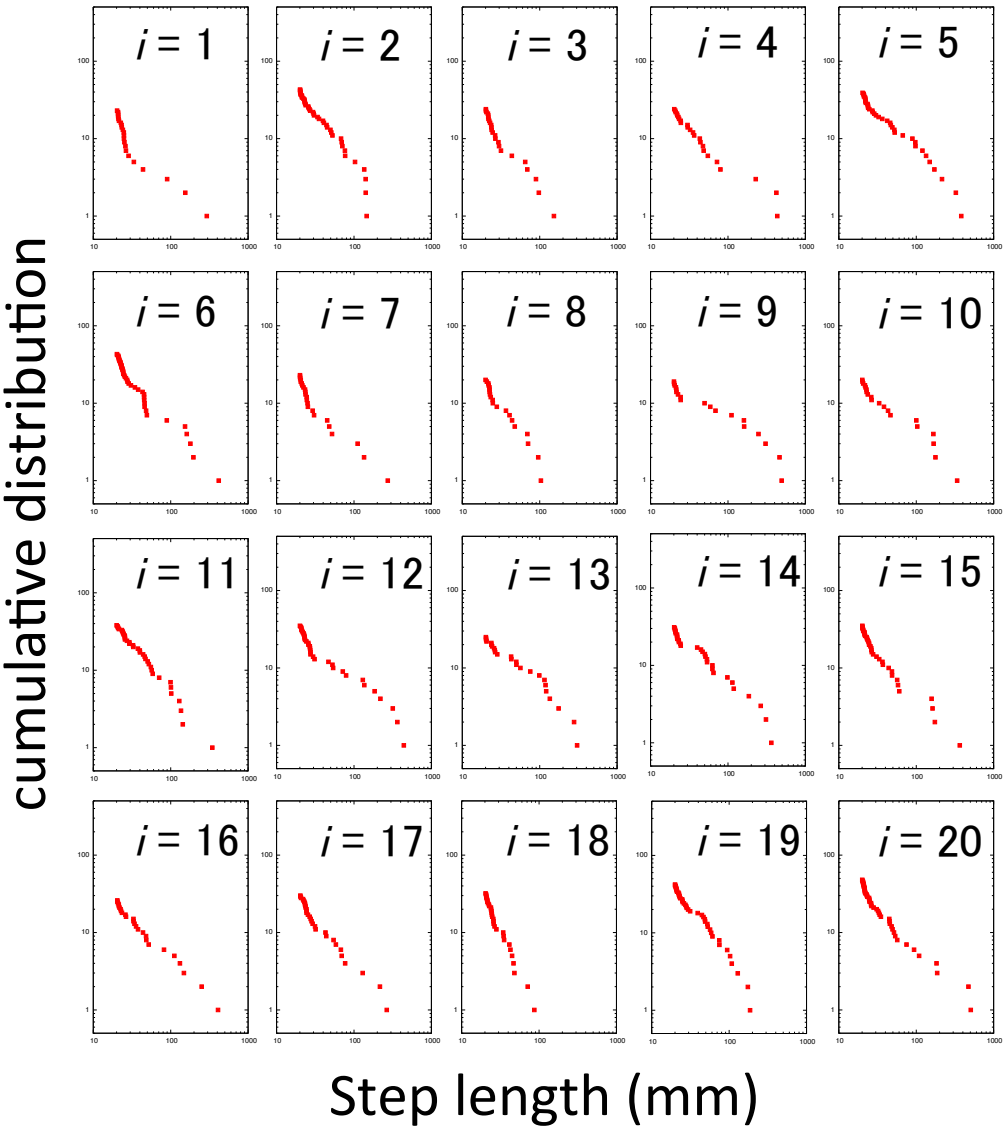

Figure 8. Cumulative distributions of step-lengths in the center of mass reference frame, displayed by each individual fish belonging to 20 individuals school. Number *i* in each plot indicates individual number that corresponds as in table 3.

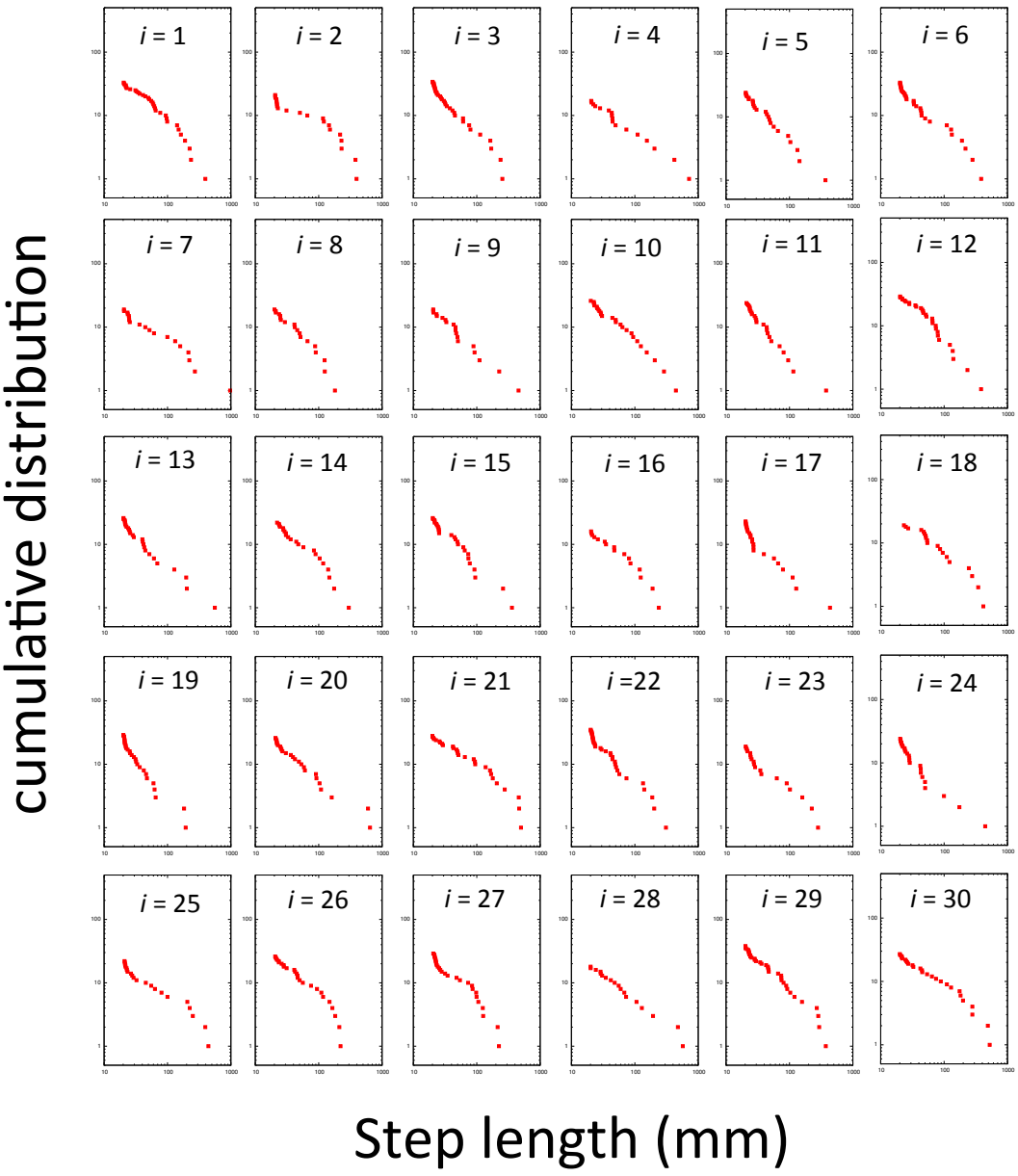

Figure 9. Cumulative distributions of step-lengths in the center of mass reference frame, displayed by each individual fish belonging to 30 individuals school. Number *i* in each plot indicates individual number that corresponds as in table 4.

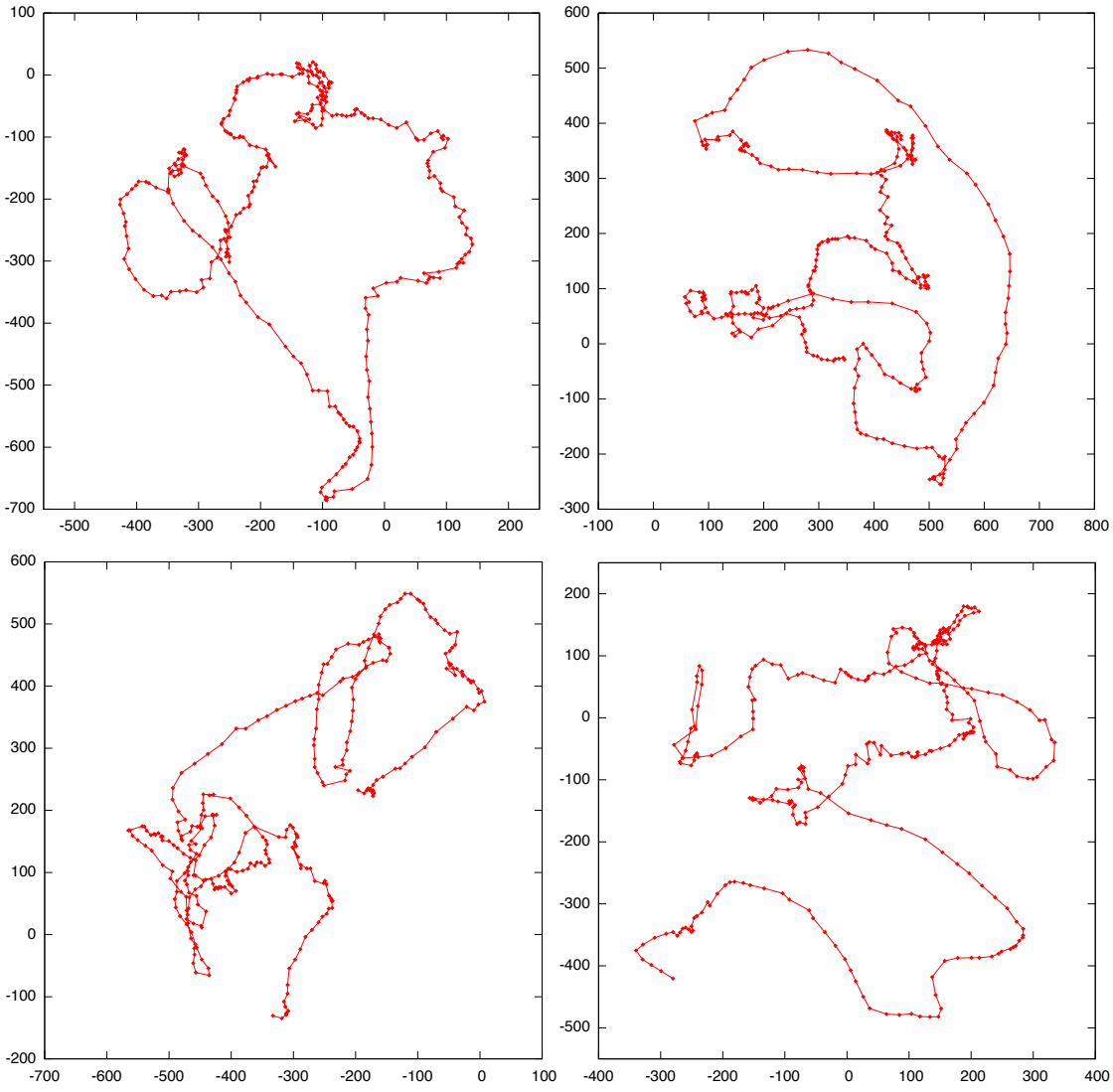

Figure 10. Trajectories of four individual fish in the center of reference frame. The axes are in millimeters.

i	***N***	***w*(*p*)**	***μ***
1	99	1.00	2.99
2	96	1.00	2.93
3	104	1.00	3.06
4	137	1.00	3.07
5	129	1.00	2.84
6	110	1.00	3.08
7	132	1.00	3.12
8	144	1.00	2.87
9	106	1.00	2.98
10	102	1.00	2.78

Table 2. Data for distributions of step-lengths in the center of mass reference frame, displayed by each individual fish belonging to 10 individuals school, where *i* indicates individual number that corresponds as in figure S1, *N* represents the total number of step-lengths, $w(p)$ is AIC weights of power-law and μ is power-law exponent.

i	N	$w(p)$	μ
1	26	0.99	2.16
2	43	0.99	2.64
3	24	0.99	3.13
4	24	0.99	2.27
5	39	0.99	2.27
6	43	1.00	2.71
7	23	0.99	3.04
8	20	0.89	2.94
9	19	0.99	1.88
10	20	0.99	2.22
11	38	0.99	2.34
12	35	1.00	2.30
13	25	0.97	2.05
14	31	0.99	2.18
15	34	1.00	2.76
16	26	0.99	2.33
17	30	0.99	2.66
18	32	0.93	3.88
19	41	0.99	2.56
20	48	1.00	2.69

Table 3. Data for distributions of step-lengths in the center of mass reference frame, displayed by each individual fish belonging to 20 individuals school, where i indicates individual number that corresponds as in figure S2, N represents the total number of step-lengths, $w(p)$ is AIC weights of power-law and μ is power-law exponent.

i	*N*	*w*(*p*)	*μ*	*i*	*N*	*w*(*p*)	*μ*
1	33	0.70	1.95	16	16	0.64	2.03
2	21	0.99	1.89	17	22	0.99	2.77
3	34	0.99	2.49	18	19	0.33	1.82
4	17	0.99	1.89	19	29	0.99	3.04
5	24	0.99	2.31	20	26	0.97	2.16
6	33	0.99	2.36	21	28	0.97	1.79
7	19	0.99	1.90	22	35	0.99	2.53
8	19	0.58	2.22	23	19	0.99	2.33
9	19	0.99	2.14	24	24	0.99	2.71
10	26	0.99	2.02	25	22	0.99	2.07
11	24	0.99	2.54	26	26	0.77	2.06
12	29	0.46	2.00	27	29	0.99	2.33
13	26	0.99	2.39	28	18	0.99	1.88
14	22	0.89	2.14	29	38	0.99	2.13
15	26	0.99	2.27	30	27	0.99	1.85

Table 4. Data for distributions of step-lengths in the center of mass reference frame, displayed by each individual fish belonging to 30 individuals school, where *i* indicates individual number that corresponds as in figure S3, *N* represents the total number of step-lengths, $w(p)$ is AIC weights of power-law and μ is power-law exponent.

2.4. Discussion

We conducted three investigations on the inherent noise in schools of ayus that show polarized and milling patterns and exhibit individual temporal coordinates. First, we calculated the mean-square displacement in the center of the mass reference frame, as seen in starling flocks, and observed that there were super-diffusive behaviors in polarized schools with exponents of $\alpha>1$. This result indicates that fish in schools diffuse faster than Brownian motion. Although model simulations have predicted two-dimensional super-diffusion with an exponent of $\alpha=4/3$ [66], diffusion in real schools occurs faster than predicted, except for schools with 10 individuals. Moreover, we observed the trend that the larger the school size is, the higher the diffusion exponent will be. This relation may be caused by an effect of the area in which the fish can travel, i.e., on the domain covered by a school. If a fish moves beyond the domain, it would be separated from its school. We might, therefore, consider that the smaller the school size is, the more constraints there will be on an individual's diffusion and that the exponent would reach a certain value in larger schools.

The polarized and milling patterns are known as emergent collective ordered states in fish schools, which co-exist for the same individual behaviors [23]. One can discriminate these two self-organized patterns by using two order parameters: polarization parameters and rotation parameters. This condition raises the question as to what type of properties would be commonly observed in both polarized and milling states. For these two states, we calculated pair-wise contact duration, which allows us to quantify neighbor shuffling because it measures how long individuals interact with neighbors. We found that the distributions of contact duration in polarized schools followed a power law, as has been observed in various human communities. This result indicates the absence of a characteristic scale with respect to how long individuals interact with neighbors. Similarly, we observed a power-law distribution in contact duration in the milling school. Therefore, this property of neighbor changing with respect to time is considered to be common both in polarized and milling patterns in fish schools. Note that the way we quantified neighbor shuffling here is different from the method employed by Cavagna and others for starling flocks. They defined neighbors as a number of individuals nearest to a focal individual, whereas we defined neighbors as individuals in the neighborhood of the focal individual within detection range r_d. In other words, whereas Cavagna and others used topological neighborhoods in their studies, we used metric neighborhoods to estimate neighbor shuffling [14].

It seems that if individuals behave ideally, there is no inherent noise and hence no position changing in the collective group. The results discussed above, however, indicate that individuals exhibit super-diffusive behavior within the group, leaving neighbors with no characteristic time scale. Such inherent noise, which might be expected to be detrimental for collectivity, plays an important role in facilitating interactions with various neighbors and thereby robust collective motion and information transfer. Is there a balance between excessive movement that is detrimental to the maintenance of the group and movement that is too slight to contribute to collectivity?

In considering this question, our results show that fish movement lengths in schools follow a power-law distribution, i.e., a Lévy walk. In a study on foraging strategy, a Lévy walk with the power-law exponent μ ranging from $1<\mu\leq3$ was considered to be important in a natural environment in which resources are unpredictably distributed [44]. A Lévy walk with $\mu=2$ indicates optimal searching

behavior in such an environment. For the exponent $\mu \approx 1$, movement patterns are close to ballistic motion. This movement is useful to a foraging animal that is exploration foraging if resources are homogeneously distributed far from an animal's location. For $\mu > 3$, the walk is approximated as Brownian motion. This motion is applicable for exploitation foraging if resources are abundantly distributed near an animal's location. A Lévy walk with the exponent μ ranging from $1 < \mu \leq 3$, therefore, indicates a foraging pattern that balances exploitation and exploration foraging.

We can paraphrase these explanations regarding individual movements within a group with an analogy. If the step lengths of individuals in the center of the reference frame follow the power-law distribution with the exponent $\mu \approx 1$, they might move with much longer step lengths that might be detrimental to collective motion and information transfer through the group. If $\mu > 3$, individuals might stay in a local region within the group, and it would be difficult for individuals' movements within the group to contribute to dynamic collective behavior. A Lévy walk with exponent μ ranging from $1 < \mu \leq 3$ was observed in schooling ayus, which can be regarded as a well-balanced movement to facilitate dynamic collective motion and information transfer throughout the group.

3. Emergent Behavior in a Swarm of Soldier Crabs Described by Inherent Noise

3.1 Background

Emergent behavior that brings about a mass effect is one of the most striking aspects of collective animal groups. In recent years, developments in image analysis have made it possible to obtain kinetic data on the movements of real organisms [15,16,24,25] and to compare that data with simulation models [28,29]. In contrast, there are few comparisons between these models and data obtained using behavioral experiments [26,30]. Rather, many behavioral experiments that have used animal groups were conducted in the context of social learning and/or the opposed relationship between an individual and society, such as that between a fish and a school [31-33]. Investigating such a behavior, however, must help to find new mechanisms underlying interactions between individuals.

Berdahl and colleagues [30] used schooling fish, taking advantage of the avoidance of light areas (or preference for darker area such as the habitat under the lee of a rock) as one approach to the problem of linking experimental behavior results to modeled behavior. In this experiment, a temporally changing light field that controlled the mean light level was projected onto a tank in which the fish were swimming. They found that if the size of the school became larger, the level of performance in a dark area increased. In short, collective sensing against light areas was enhanced in larger schools. Moreover, by comparing this with the model, they concluded that this situation arose from the rule of attraction that has been proposed in some theoretical models such as BOIDS [7] and the zone-based model [18] by which an agent approaches neighbors if they are separated from each other. This raises the question of cases of spontaneously invading an avoidance area, which are frequently found in biology. [34,35] In this case, it would be expected that a different rule from the attractive explanation is required.

In this study, we conducted an experiment with respect to invading avoidance areas using a swarm of soldier crabs, *Mictyris guinotae* [36-39], which live in the tideland and can form large swarms. Through numerous field surveys of soldier crabs, we found the following observations to be characteristic of soldier crab general swarming behavior: (i) A swarm moving in the tideland has inherent noise. In other words, crabs have different velocities in maintaining a directed swarm, which reveals the local turbulent flow in a swarm. (ii) When a swarm faces a pool that has been naturally generated on a tideland, it does not enter this avoidance area if the swarm is small or sparse. In contrast, if the swarm becomes bigger and forms a dense region, this part of the swarm rushes into the pool without pausing. In other words, turbulent motion results in part of the swarm becoming highly concentrated, and this part enters and crosses the water due to the effect of the group. (iii) Individuals in other parts of the swarm follow their predecessors.

Based on these observations, in particular observation (ii), we designed an experiment for the water crossing behavior of soldier crabs, *M. guinotae*. To investigate the behavior, we created an apparatus with a water pool sandwiched between two shore areas under semi-natural conditions and made comparisons between small (5 individuals) and large (15 individuals) swarms with respect to the

performance of water crossing behavior. Then, we estimated whether the performance changed depending on the size of the swarm concentrated at the edge of the water pool. Finally we compared the experimental results with a swarm model based on inherent noise that was proposed in our previous study [22, 40-42].

3.2. Materials and Methods

3.2.1. Soldier Crabs *Mictyris guinotae*

We studied *M. guinotae* living in Funaura Bay on Iriomote Island, Okinawa Prefecture, Japan. Soldier crabs, whose carapace sizes are approximately 15 mm, are among the few crabs adapted to walking forwards, rather than sideways [36-39]. Although they burrow tunnels and live under substrate at higher tidal levels, they emerge and feed on detritus on the lagoon surface in swarms at the lower tidal level. During the breeding season (from December to March), their behavior differs depending on mating [67]. To avoid these effects, our experiment was conducted in the daytime during the 4 hours around ebb tide on fine weather days in October 2013. Crabs were collected in plastic containers that contained mud substrate and were separated into each swarm size in the 5 minutes before each trial. For each trial different swarm composed of different crabs were used without pre-training, with a total of nine hundred crabs used throughout the experiment. Crabs were immediately released after the experiment. No specific permits were required for the described field studies and the locations are not privately-owned or protected in any way. *M. guinotae* is not endangered or protected species.

3.2.2. Experimental Setup

A simple apparatus was constructed on the tideland (figure 10). We formed a rectangle by inserting plastic plates vertically, 100 mm deep into a flat area on the tideland (300×900 mm, 100 mm height). To make a pool (300×300 mm, 15 mm depth) sandwiched between two shore areas, we dug out the central part of the tideland surrounded by the plates and covered the rectangular area with a vinyl sheet onto which some mud was added. The pool was then filled with water obtained from a naturally generated pool. The vinyl sheet was used to inhibit crabs from burrowing tunnels and to keep the water in the pool. The crabs did not burrow tunnels during any trials and the water level changed little. Before each trial, we leveled the shore areas and resupplied water to the pool to maintain conditions.

Each swarm was gently thrown onto one side of the shore area apparatus, and swarm behavior was recorded for three minutes with a video camera (Panasonic HDC-TM700, 1920×1080 pixels). We used image-processing software (ImageJ; Rasband, W.S., National Institutes of Health, Bethesda, Maryland, USA) to calculate inter-individual distances (at 3 seconds intervals). We obtained x–y coordinates for each crab as a single pixel whose side length was 0.56 mm.

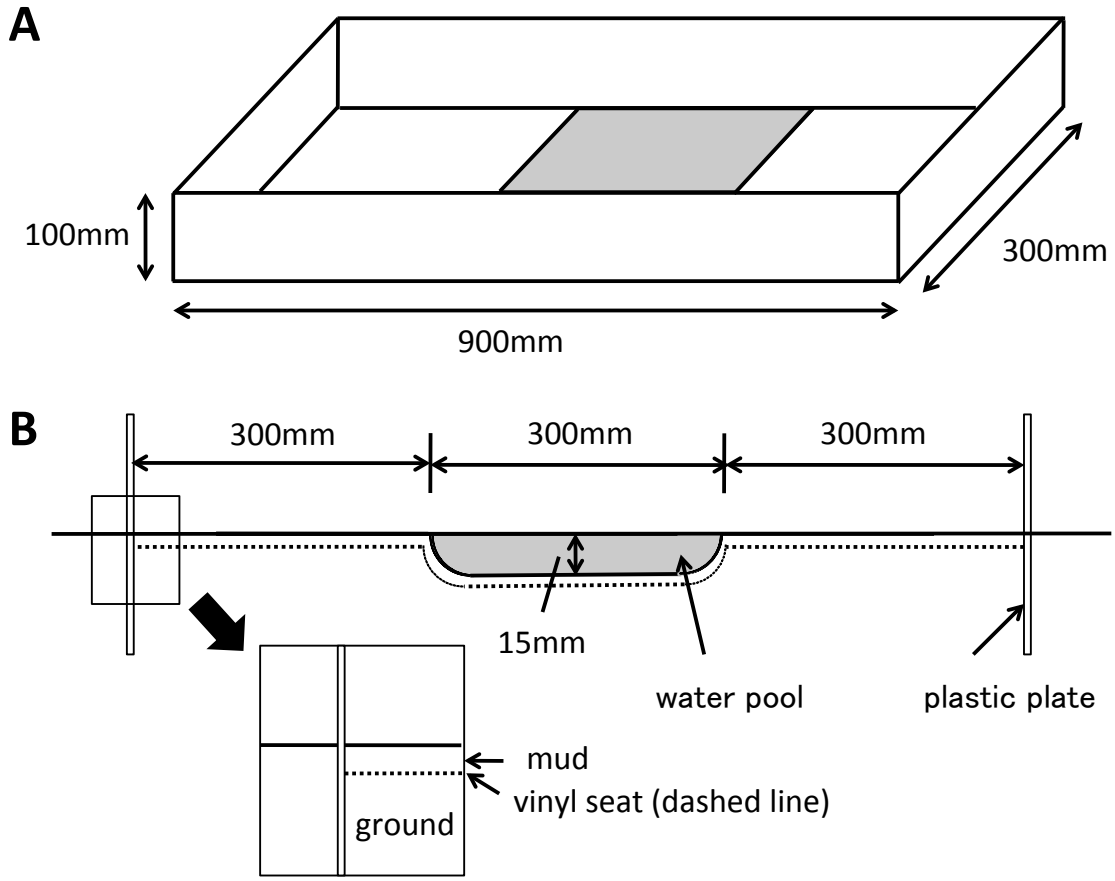

Figure 10. (A) Experimental apparatus for water crossing behavior. Plastic plates surround the tidal land to form a rectangular shape. The pale grey areas represent the water pool. (B) Cross section of apparatus. The water pool is sandwiched between two shore areas.

3.2.3. Swarm Model

Here we describe our swarm model in detail. We present a rough idea of the model in the results section.

Firstly, we describe basic behavior of the model.

Our swarm model consists of *N* individuals moving in discrete time and in a discrete $S \times S$ space where $S = \{1,2, \ldots, s_{MAX}\}$. The location of the *k*-th individual at the *t*-th step is given by

$$\boldsymbol{P}(k,t) = (x,y) \quad , \qquad (1)$$

where $x \in S, y \in S, k \in K = \{1,2, \ldots, N\}$, and the boundary condition is given as wrapped fashion. Each *k*-th individual at the *t*-th step has *P* number of potential vectors $\boldsymbol{v}(k,t;i)$ with $i \in I = \{0,1, \ldots, P-1\}$. If $i = 0$, the vector $\boldsymbol{v}(k,t;0)$, called the principal vector, is represented by the angle $\theta_{k,t}$, such that

$$\boldsymbol{v}(k,t;0) = (Int(L\cos\theta_{k,t}), Int(L\sin\theta_{k,t})) \quad , \qquad (2)$$

where for any real number x, $Int(x)$ represents integer X such that $X < x < X+1$. L is the length of principal vector. Because of the wrapped fashioned boundary condition, $X \in S$. If $i \neq 0$, the vector is defined using a random value, η, selected with equal probability from [0.0, 1.0] and a random value (radian), ξ, selected with equal probability from $[-\alpha\pi, \alpha\pi]$, as

$$\boldsymbol{v}(k,t;i) = (Int(L\eta\cos(\theta_{k,t}+\xi)), Int(L\eta\sin(\theta_{k,t}+\xi))) \, . \qquad (3)$$

The principal vector $\boldsymbol{v}(k,t;0)$ is a special case where $\eta = 1.0$ and $\xi = 0.0$. For each $\boldsymbol{v}(k,t;i)$, the target of the vector is represented by $\boldsymbol{\tau}(k,t;i)$ such that

$$\boldsymbol{\tau}(k,t;i) = \boldsymbol{P}(k,t) + \boldsymbol{v}(k,t;i) \quad . \qquad (4)$$

To implement mutual anticipation, we define the popularity of the targets of the vectors. The popularity is defined for each site at the t-th step, (x, y) with $x \in S, y \in S$, by

$$\zeta(x,y;t) = \left| \{ \boldsymbol{\tau}(k,t;i), k \in K, i \in I \mid \tau(k,t;i) = (x,y) \wedge {}^{\forall}(k \in K)\boldsymbol{P}(k,t) \neq (x,y) \} \right| \, . \qquad (5)$$

Before updating the location, for any (x, y) at the t-th step, we set

$$\omega(x,y;t) = 0 \quad . \qquad (6)$$

Updating the location of individuals is asynchronously executed. The order of updating is randomly determined independent of the number of individuals, k. If there exists $i \in I$ such that

$$\zeta(\boldsymbol{\tau}(k,t;i)) > 1 \quad , \qquad (7)$$

the next site for the k-th individual is defined by

$$\boldsymbol{P}(k,t+1) = \boldsymbol{\tau}(k,t;s) \quad , \qquad (8)$$

where s satisfies the condition such that for any $i \in I$,

$$\zeta(\boldsymbol{\tau}(k,t;s)) \geq \zeta(\boldsymbol{\tau}(k,t;i)) \quad . \qquad (9)$$

In other words, an individual moves to the target of its own potential vector that has maximum popularity. If there multiple sites satisfy condition (9), one of them is chosen randomly.

Because updating is asynchronous, a set of sites updated by equation (8) is gradually grows. A set of updated sites is represented by $U_N = \{(x,y) \in S \times S \mid \boldsymbol{P}(k,t+1) = (x,y)\}$.

An individual that satisfies condition (7) and moves by equation (8) is called a wanderer. The vacated site generated by a moving wanderer is recorded in memory by

$$\omega(x,y;t) = 1, \text{ if } \boldsymbol{P}(k,t) = (x,y) \wedge \boldsymbol{P}(k,t+1) \in U_N \quad . \tag{10}$$

After all wanderers have been updated, an individual which does not satisfy condition (7) moves to the vacated site in follower-neighborhood, N_f, by

$$\begin{aligned} &\boldsymbol{P}(k,t+1) = Rd\{(x,y) \in N_f \mid \omega(x,y;t) = 1\}, \\ &\text{if } \left|\{(x,y) \in N_f \mid \omega(x,y;t) = 1\}\right| \geq 1 \end{aligned} \quad , \tag{11}$$

where RdJ represents an element randomly chosen from set J. An individual whose movement is determined by equation (11) is called a follower.

If an individual is neither wanderer nor a follower, it moves by

$$\begin{aligned} &\boldsymbol{P}(k,t+1) = \\ &Rd\{\boldsymbol{\tau}(k,t;i) \mid {}^{\forall}(j \in K')\boldsymbol{P}(j,t) \neq \tau(k,t;i) \wedge \tau(k,t;i) \notin U_N\} \end{aligned} \quad , \tag{12}$$

where K' is an index set of individuals that are not updated.

Finally, principal vectors are locally matched with each other in the neighborhood through velocity matching, M. This matching operation is expressed as

$$\theta_{k,t+1} = \left\langle \theta_{k,t} \right\rangle_M \quad . \tag{13}$$

The bracket with M represents the average velocity direction in the neighborhood, M. The parameters in our model are listed below.

L : the length of principal vector
P : number of potential vectors
α : angle derived from the principal vector

R_f : radii of the follower-neighborhood

R_M : radii of the neighborhood of velocity matching

Secondly, we define water crossing behavior in our model.

In the simulation introducing the pool, we define a specific area $U_p \subseteq S \times S$ in which the condition (7) that allows mutual anticipation (equation (8)) is replaced by

$$\zeta(\boldsymbol{\tau}(k,t;i)) > c \,. \qquad (14)$$

In the simulation, we set at $c = 2$. Hence, it is more difficult for individuals to go through the area U_p, which mimics a water pool that an individual soldier crab does not enter. Only by introducing the specific area U_p, can we simulate the water crossing behavior.

Finally, we show tendency to walk along a wall in our model.

We first define the wall state for any lattice (x, y) such that

$$w(x,y) = \begin{cases} 1, & \text{if the site is the wall state;} \\ 0, & \text{otherwise} \end{cases} . \qquad (15)$$

In the simulation of water crossing behavior, an agent can be located only at a site where $w(x,y) = 0$. The angle of tangential direction is defined for each wall state site (x, y) and is represented by $\theta_w(x, y)$. The tendency of walking along a wall is defined by

$$\theta_{k,t} = Rd\{\beta, \beta + \pi\} \quad , \qquad (16)$$

$$\beta = Rd\{\theta_w(x,y) \mid d(\boldsymbol{P}(k,t),(x,y)) \le d(\boldsymbol{P}(k,t),(u,v)), \; w(x,y) = w(u,v) = 1, (x,y),(u,v) \in N_W\} \quad , \qquad (17)$$

where $d((p, q), (x, y))$ represents the metric distance between two sites (p, q) and (x, y), and N_W represents the neighborhood of wall-monitoring for each agent with a radii $R_w = 2$. If an agent is close to the wall with respect to N_W, the agent's velocity, $\theta_{k,t}$ is parallel to the tangential direction of the wall. After this operation, velocity matching (equation (13)) is applied to all agents. Only from (16) and (17) can agents close to the wall walk along the wall.

3.3. Results

3.3.1. Experimental Results

To investigate whether the water crossing behavior was caused by mass effect, we compared small swarms (5 individuals) with large swarms (15 individuals) with respect to the performance of water crossing behavior. Each trial was conducted for three minutes and a total of 40 trials were performed for each swarm size. For each trial, the success rate φ was defined by the number of individuals that completely walked across the water pool, normalized by the total number of individuals. The success rate φ was zero if no crabs completely walked across the pool, while it was one if all of the crabs finished crossing to the opposite shore. According to field observations of naturally generated water crossing behavior, there were some crabs left in the water pool, so not all individuals composing the swarm finished crossing to the other shore. Hence, we defined a success trial by $\varphi > 0.5$, a failure by $\varphi \leq 0.5$, and the performance of water crossing behavior by the number of success trials normalized by the total number of trials.

Figure 11 shows the performance of water crossing behavior and the frequency of successful and unsuccessful trials. The performance differed significantly between small and large swarms (performance: 30/40 (large swarm) vs. 10/40 (small swarm), Fisher exact test: $P < 0.001$). The number of failed trials performed by small swarms was significantly larger than the number of successful trials (failure trial: 30 out of 40 swarms, binomial test: $P < 0.01$). The number of successful trials performed by large swarms was significantly larger than the number of failures (success trial: 30 out of 40 swarms, binomial test: $P < 0.01$). These results indicate that while small swarms avoid entering the water, large swarms cross over the water pool. This can be interpreted as emergent behavior caused by a mass effect.

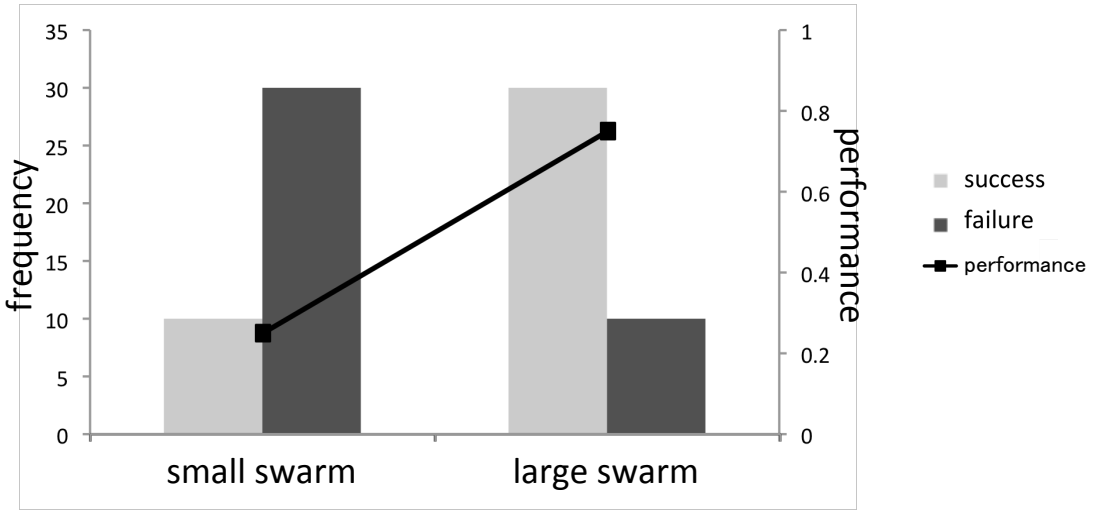

Figure 11. Frequency of success and failure as well as performance of each water crossing behavior. Large swarm, $N = 40$; small swarm, $N = 40$.

Detailed results of the above analysis that show the success rate φ and *NI* of each trial are provided in Table 1. *NI* indicates the number of individuals that eventually crossed the pool during a trial. Between small and large swarms, we found a significant difference in the number of trials in

which no crab crossed the river (0/40 (large swarm) vs. 14/40 (small swarm), Fisher exact test: $P < 0.001$). This result shows that small swarms avoid the water. There is, however, no significant difference in the number of trials in which all crabs finish crossing to the opposite shore (7/40 (large swarm) vs. 2/40 (small swarm), Fisher exact test: $P > 0.05$, NS), which means that crabs composing the swarm do not always finish crossing, independent of swarm size, as seen in natural conditions.

Small swarms							Large swarms					
Trial	ϕ	***NI***	**Trial**	ϕ	***NI***		**Trial**	ϕ	***NI***	**Trial**	ϕ	***NI***
1	0	**0**	21	0.2	1		1	0.6	9	21	0.73	11
2	0.8	4	22	0	**0**		2	0.87	13	22	0.87	13
3	1	**5**	23	0	**0**		3	0.67	10	23	0.93	14
4	0.2	1	24	0.6	3		4	0.67	10	24	0.67	10
5	0.6	3	25	0.4	2		5	0.87	13	25	0.87	13
6	0.8	4	26	0.2	1		6	1	**15**	26	0.27	4
7	0.6	3	27	0.2	1		7	1	**15**	27	0.33	5
8	0.8	4	28	0.4	2		8	1	**15**	28	0.2	3
9	0.2	1	29	0.4	2		9	1	**15**	29	1	**15**
10	0	**0**	30	0	**0**		10	0.93	14	30	0.93	14
11	0	**0**	31	0.2	1		11	1	**15**	31	0.73	11
12	0	**0**	32	0.6	3		12	0.2	3	32	0.73	11
13	0.2	1	33	0	**0**		13	1	**15**	33	0.67	10
14	0.2	1	34	0	**0**		14	0.73	11	34	0.07	1
15	0.4	2	35	0	**0**		15	0.6	9	35	0.4	6
16	0.2	1	36	0	**0**		16	0.6	9	36	0.27	4
17	0	**0**	37	0.4	2		17	0.67	10	37	0.73	11
18	0.2	1	38	0	**0**		18	0.8	12	38	0.4	6
19	0	**0**	39	0.2	1		19	0.47	7	39	0.87	13
20	1	**5**	40	0.8	4		20	0.33	5	40	0.87	13

Table 5. Detailed results for the analysis shown in figure 11. The success rate ϕ was defined by the number of individuals that completely walked across the water pool during each trial, normalized by the total number of individuals. *NI* indicates the number of individuals that eventually crossed the pool during each trial.

To estimate the contribution of the density effect on the water crossing behavior in detail, we investigated whether the performance depended on the size of the swarm concentrated at the edge of the water pool. First, to equalize the conditions when the swarm entered the water, we defined the initial condition such that there was no crab in either the pool or on the opposite shore area at a certain time

step and that in the next time step a crab entered the pool. Note that we only used crab positional data at each of the time steps, which were separated by three seconds intervals, and ignored crab behavior between time steps. Second, to calculate the size of the swarm concentrated at the edge of the pool, we defined the swarm network as a swarm that consisted of individuals within 50 mm of another individual; such individuals were connected to each other as the nodes of the network. We calculated the size of the swarm network that a crab entering into the pool belonged to and checked the performance for each swarm network. As long as it satisfied the initial condition, we continued to check the performance for each swarm network until each trial finished. In this analysis, we defined a failure trial as a trial in which all individuals comprising a network did not finish crossing the pool and a successful trial as a trial in which at least one individual within the network completely walked across the water pool. The performance of water crossing behavior was defined as the number of successful trials normalized to the total number of trials. Figure 12A and B show the performance of water crossing behavior and frequency of success as well as the failure of small and large swarms, respectively. It is easy to see that the smaller network size was (in particular when the network size was one), the smaller the performance was for both small and large swarms. When the network size was more than six, every swarm successfully crossed the water. When we compiled the data sets for both large swarms and small swarms, we found significant differences in the performance between solitary crabs (i.e., network size is one) and swarms with network sizes that were greater than two (performance; 53/76 (swarm) vs. 22/70 (solitary crab), Chi-square test: $\chi^2_1 = 19.900$, $P < 0.001$) (figure 12C).

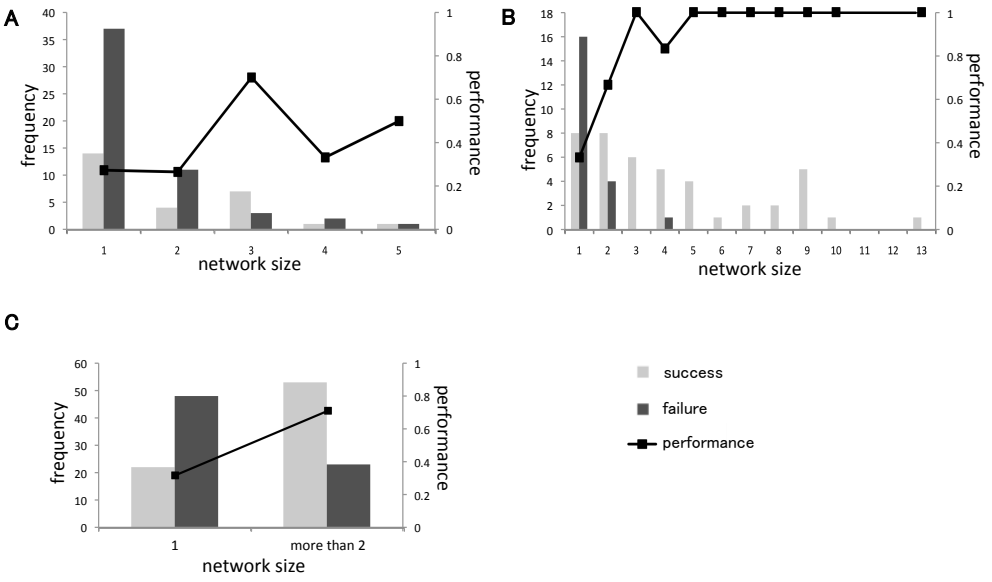

Figure 12. (A) Frequency of success and failure of each network size as well as the performance of small swarm trials, N =81. (B) Frequency of success and failure of each network size as well as the performance of large swarm trials, N = 65. (C) Frequency of success and failure as well as the performance of solitary crabs (i.e., network size is one) (N = 70) and a swarm whose network size was more than two (N = 76).

Figure 13 shows typical snapshots of the water crossing behaviors with some trajectories. Each crab is represented by a different color. Trajectories are composed of small squares representing each crab's location and dashed lines that connect the locations at one time with those at the next time. The number next to each square represents the order of time, with a time interval of three seconds. The blue vertical line in figure 13A,B represents the border between the shore area and the pool area. Figure 13A provides examples of successful water crossings. It shows the effect of gathering at the edge of pool; once a swarm composed of six crabs entered into the pool, it crossed over the pool without stopping. Figure 13B provides an example of failure of the behavior. Although the crab entered the pool at least once, it hesitated in the water and left the pool. In addition, even though other crabs crossed over the pool, a crab was left in the pool, as was seen in natural conditions (figure 13C).

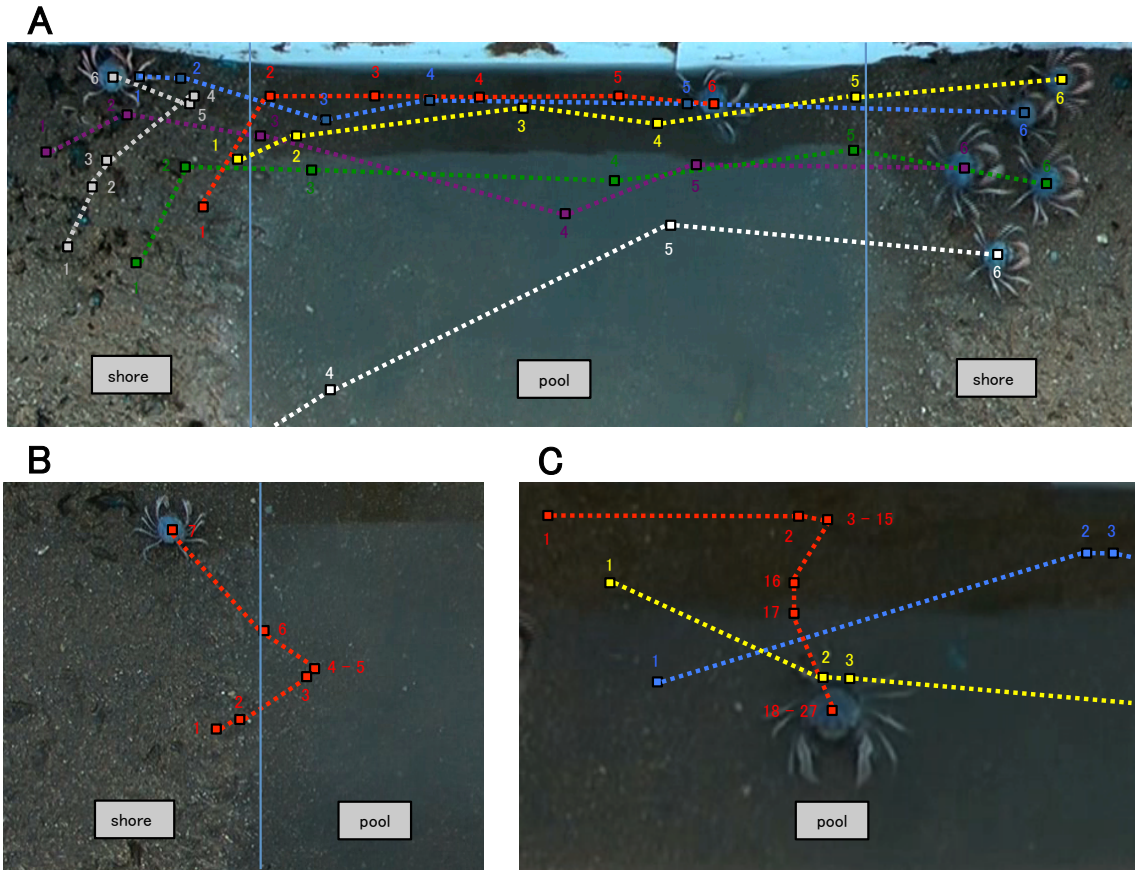

Figure 13. Typical snapshots of water crossing behavior with several trajectories. Different colors correspond to different crabs. Trajectories are composed of small squares that represent the location of each crab and dashed lines that connect its location at a certain time with its location at the next time. The number next to each square represents the order of time, with a time interval of three seconds. The shore area and pool area are divided by a blue vertical line. (A) Example of a successful water crossing. (B) Example of a failed behavior. (C) Example of a crab being left in the pool despite the crossing of the other crabs.

3.3.2. Swarm Model Based on Inherent Noise

Here, we show a swarm model to explain emergent water crossing behavior. As mentioned in the introduction section, using numerical field observations and experimental results we found the following characteristics of general swarming behavior in soldier crabs: (i) a swarm moving in a lagoon has inherent noise and maintains coherence; (ii) turbulent motion results in part of the swarm becoming highly concentrated, and this part enters and crosses the water through an effect of the group; and (iii) individuals in other parts of the swarm follow their predecessors. Characteristic (i) suggests perpetual negotiation among individuals with respect to direction. Characteristic (ii) reveals that density affects the mechanism to generate a swarm. Such an inherent noise has been found not only in the swarming of soldier crabs but also in other animal groups. For example, in a starling flock each bird continuously changes its neighbors and reveals supper-diffusive behavior in the center of the mass reference frame of the flock [24]. Moreover, it has been reported that a noise inherently generated within a locust-march plays an essential role in the collective change of direction [26]. When considering (i) combined with (ii), it is suggested that inherent noise positively contributes to generate and maintain a swarm.

To incorporate these soldier crab swarm behaviors into a model, we introduced several potential transitions for each individual that allowed the individual to anticipate the movements of other individuals within the swarm (figure 14A). Each individual has its own principal vector (velocity) accompanied by a number of potential transitions (P) in a range restricted by the angle (α) and the length (L). If the targets of any potential transitions overlap at a certain site (lattice), the number of potential transitions to that site is counted as the site's "popularity". If there are multiple sites with a popularity larger than 1 (threshold value) among an individual's potential transitions, it is assumed that the individual moves to the site with the highest popularity. If several individuals intend to move to the same site, one individual is randomly chosen to move there and the others move to their second most probable site. This rule represents the mutual anticipation of the individuals. For example, people often manage to avoid collisions and walk in a crowd of others using anticipation [68,69]. Therefore, we implement this type of behavior into our model. If there is no site with a popularity exceeding the threshold value in the neighborhood of an individual, and if others within a radius R_f move due to mutual anticipation, the individual moves to occupy the absent site generated by mutual anticipation. Namely, it follows its predecessor. If an individual's movements are not based on mutual anticipation or the actions of a predecessor, it moves in the direction of a randomly chosen potential transition. This type of individual is called a "free wanderer" (see further details in Materials and Methods).

We implemented these rule in an asynchronous updating model in a lattice space coupled with velocity matching (VM) of principal vectors (figure 14A). VM is implemented in a neighborhood with a radius R_M. By assuming a maximum of one individual per lattice, the model implements collision avoidance (CA). The predecessor-following rule is also an example of flock centering (FC) (also known as attractive rule). The rules of VM, CA, and FC constitute BOIDS. BOIDS has recently been expanded to model more realistic characteristics of flocks and schools [18-21,70]. Thus, the introduction of mutual anticipation to our model is a natural extension of BOIDS. Figure 14B demonstrates how various swarming patterns in the model with rapped boundary conditions depend on the parameters α and P with $R_f = 2$ and $R_M = 3$. If P is 1, the model mimics BOIDS. If P is 2, multiple potential transitions

break out in collective motion because two transitions contribute not to make a popular site, but to make a random transition. If P exceeds 2, mutual anticipation contributes to swarm formation, especially if α is large. It is easy to see that a swarm contains turbulent motion despite maintaining a highly dense whole when P is larger. Furthermore, if there is a solitary individual, it is regarded as a free wanderer and moves by choosing randomly from potential transitions. Therefore, the larger P is, the more random an individual's move is. In this sense, we can regard potential transitions as inherent noise. In our previous study, we showed that this model could explain several phenomena exhibited by animal groups [22, 40-42].

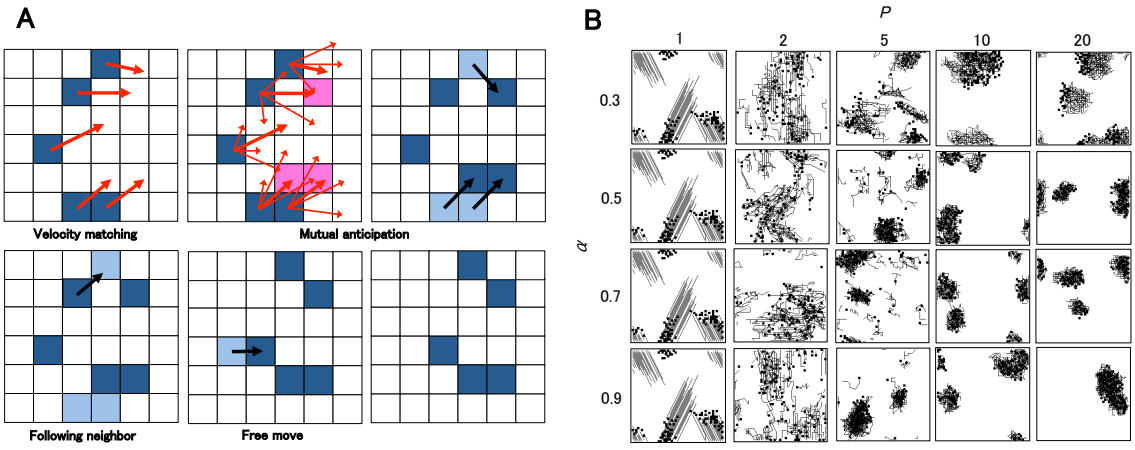

Figure 14. Schematic diagram of the model and the behavior of a model simulation. (A) Illustration of a transition of a swarm in lattice space. Each individual is represented by a blue cell and their potential transition is represented by a red arrow. The principal vector is represented by a thick red arrow. First, velocity matching is applied to the principal vectors (upper left). Next, the mutual anticipation is estimated. The amount of overlap between targets of potential transitions is calculated and sites with an overlap larger than 1 (threshold) are obtained (pink site). For example, the popularity of the highest pink site is 2 (upper center). An individual whose potential transitions reach some popular sites moves to the most popular site (black arrow in the upper right). After that, followers (lower left) and free wanderers (lower center) move, which results in the final distribution (lower right). (B) How changing P and α affects the patterns of a swarm composed of 100 individuals in a 50×50 lattice. Each individual is represented by a square and a trajectory tail, where L=4, R_f = 2, and R_M = 3.

3.3.3. Water Crossing Behavior in the Swarm Model

In this section, we show the water crossing behavior performed by our swarm model, setting the parameters at P =10, α =0.5, L = 4, R_f = R_M = 2. Emulating the experiment conducted with real swarms, we set the bounded space to consist of 90×30 lattices in which the pool area (30×30 lattices) was sandwiched between the shore areas (each 30×30 lattices). The pool, as an avoidance area, was defined as a specific area in which the condition allowing mutual anticipation of potential transitions

were overlapped larger than two (see Materials and Methods). Hence it was more difficult for individuals to go through the specific area, which mimics a natural pool that an individual soldier crab does not enter. In this simulation, individuals could not go outside the bounded space, emulating the wall of the experimental apparatus, even though potential transitions overlapped with the area outside of the space. In addition, individuals were given the tendency to walk along the boundary of the space because it has been reported that real solder crabs tend to walk along the wall (see Materials and Methods).

In each simulation, individuals were randomly allocated to one of the shore areas with random directions of principal vectors. We conducted each trial for 250 time steps and ran 100 trials for swarms with 3, 5, …, 21 individuals. Successful trials, failures, and the performance of water crossing behavior were defined by using the success rate φ along with the experiment conducted with real crabs. Figure 15 shows the performance of water crossing behavior and the frequency of success and failure for each swarm size. It is easy to see that the bigger the swarm size, the more success in water crossing. When we compared the performance between swarms composed of five (small) and fifteen (large) individuals that were compared in the real soldier crab experiment, there were significant differences between these swarms (performance: 68/100 (fifteen individuals) vs. 19/100 (five individuals), Chi-square test: $\chi^2_1 = 39.872$, $P < 0.001$).

In the experiment, because of difficulty in collecting a huge number of fresh crabs, we only tested two sizes of swarms (i.e., 5 and 15 individuals) with real crabs. However, we can predict the behavior of intermediary size of swarm by using our swarm model. In figure 15, it can be observed that the performance of water crossing behavior of our model exceeds 0.5 i.e., the number of successes is over the number of failures when the swarm size is more than nine. Hence it would be expected that if we test a swarm composed of over nine real crabs, the swarm success the water crossing behavior on more than half of trials.

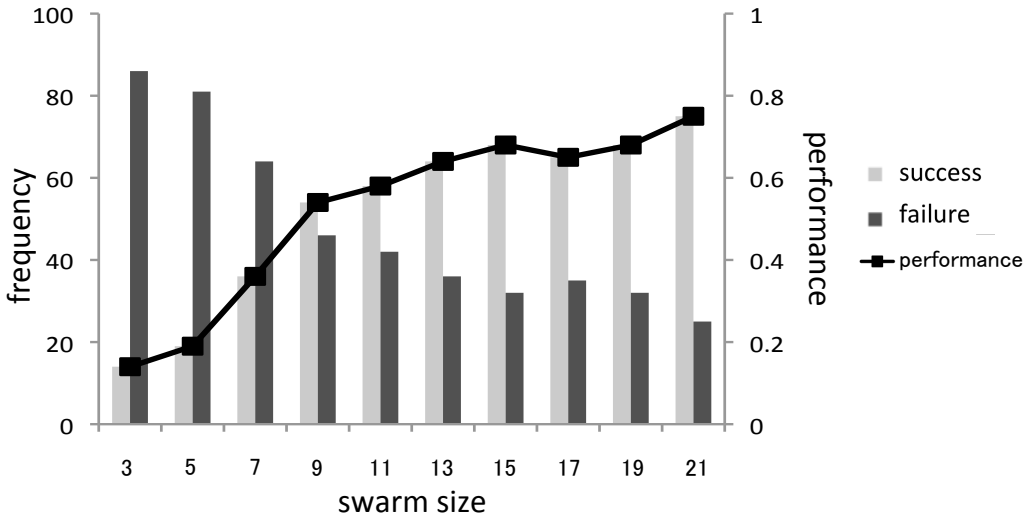

Figure 15. Frequency of success and failure as well as the performance of each swarm size (N = 100 for each swarm size). It is clear that if the swarm is bigger, the success rate of crossing the water increases.

Figure 16 shows snapshots of the time development of swarm trajectories in a model simulation. Each agent is represented with its 10-step trajectories. The pale grey area located in the center indicates the pool area in which the threshold to allow mutual anticipation is heightened. In the case of a swarm whose size is five, solitary or few individuals do not enter into the pool, even though the swarm walks along the marginal area of the pool. On the other hand, in the case of a swarm whose size is fifteen, dense swarm is formed at the edge of pool, and once individuals enter into the pool they cross over the pool without stopping. Moreover, we observed that some individuals remained in the pool despite the crossing over of the others, which is frequently observed with real soldier crabs (indicated by red circle in figure 16). Therefore, the simulated swarm appropriately mimics the behavior of real soldier crabs as shown in the experiment and natural conditions.

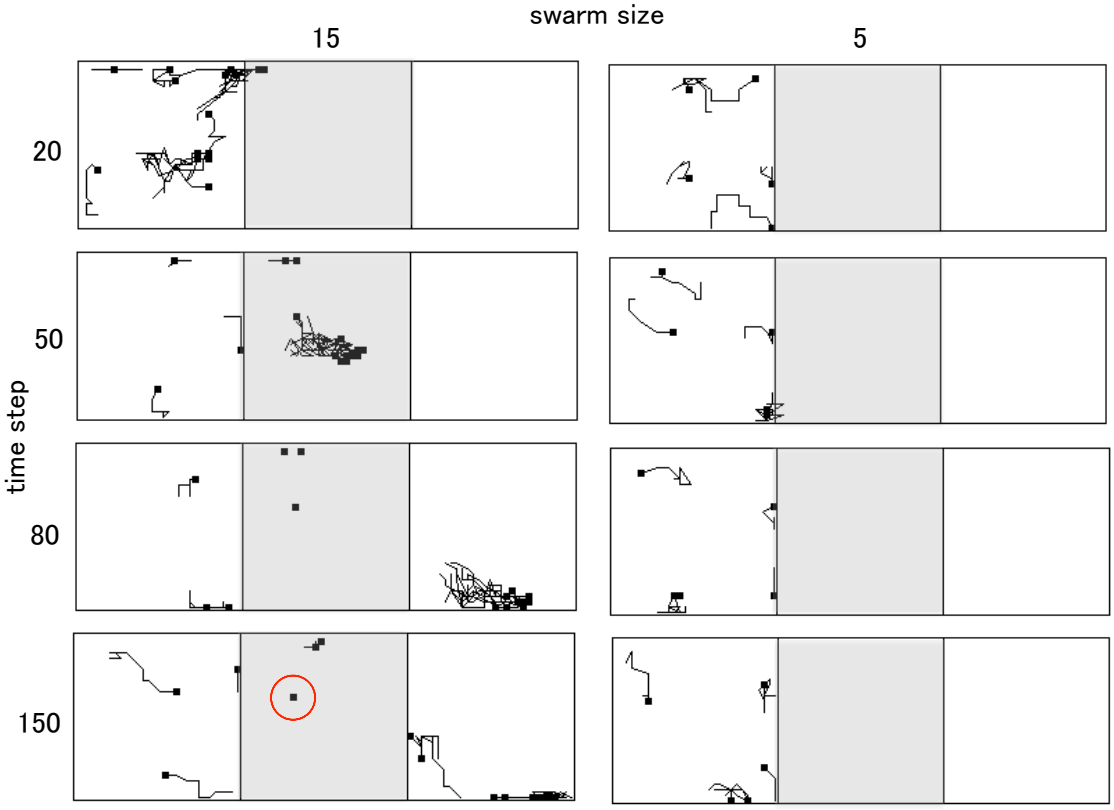

Figure 16. Snapshots of the time development of swarm trajectories in a model simulation. The pale grey area located in the center indicates the pool area. An individual left in the pool is indicated by a red circle.

3.4. Discussion

In this study, we first conducted an experiment with respect to water crossing behavior of soldier crab swarms. We observed that when a small swarm confronted a waterfront, it could not enter a water pool. Hence, when a swarm was small or sparse, they regarded the water pool as an area to avoid entering. In contrast, when the swarm became bigger and a highly concentrated part was created inside the swarm, they could then enter and cross the water. Therefore, by creating a large and dense region, the swarm could overcome the water pool as an avoidance area. Although spontaneous invading behaviors into an avoided area have been reported for several animals, in most cases, animals have some motivation such as rich food sources to encourage entrance into an avoidance area [34,35]. Our experimental results indicate that the behavior of overcoming the avoidance area observed in soldier crab swarming is obviously an emergent behavior because, while small swarms passively responds to a water pool as a noxious stimulus, if the swarm becomes bigger they spontaneously enters to the pool. Some examples of emergent behavior of collective animals were presented previously [10,30]. In particular, Berdahl and others [30] revealed that greater group-level responsiveness to the environment arises spontaneously as group size increases. For example, a fish school stays away from the light as an avoidance area more sensitively if it is bigger in size. They explain this emergent behavior by the simple rule of attraction such that an agent approaches its neighbors if they separate from each other.

The water crossing behavior can be explained by our model, which incorporated inherent noise and mutual anticipation. Inherent noise in the model created diverse potentials for each individual and the swarm collapsed if each individual chose potential transitions randomly. In contrast, if the diversity of moves is used for other individuals' anticipation, this results in a densely collective motion. Mutual anticipation may be affected by each individual crab's sensitivity to the moves of other individuals and by the asynchronous movements of the individuals in a swarm. This sensitivity allows crabs to detect the site to which many individuals could move toward. Because of asynchronous updating, crabs can move in various directions without collision and overcrowding.

By considering the water pool to be an area where it is difficult for mutual anticipation to occur, the water crossing behavior is easily simulated in our model. In simulations with small swarms, even if it is faced with the marginal area of the pool, it cannot enter the pool because potential transitions are not overlapped enough for mutual anticipation of the swarm to occur in the pool. For a large swarm, however, after regions of high concentration are formed, the swarm can enter the pool and make mutual anticipation at sites in the pool due to highly concentrated potential transitions. Then, even when an individual cannot occur due to mutual anticipation in the pool, it is not separated from swarm as long as it can follow the predecessor, and hence the swarm crosses over the pool without stopping. However, if the individual cannot use either mutual anticipation or follow its neighbors, it is separated from swarm and left in the pool, as was seen in the experiment. In this way, our swarm model can emulate the behavior of real soldier crabs to some extent. It is difficult to explain the behavior of entering an avoidance area only with the simple attraction rule because when a local part of a swarm enters into the water pool and the greater part of it stays on the shore around the pool, the local part is brought back to the greater part by following the attraction rule.

Inherent noise can be widely seen in animal groups [24,26,65,71]. By using mutual

anticipation, inherent noise that could be expected to negatively impact the swarm, makes a positive contribution to the collective motion and can explain the water crossing behavior of a soldier crab swarm. These results suggest that inherent noise and mutual anticipation play an important role in understanding collective behavior.

4. Animal Foraging Strategy

4.1 Background

It has been intriguing question how living orgasms behave to get targets in natural environment where resources are usually unpredictably distributed and thus orgasms have limited information about locations of them [43]. Lévy walk (LW) is considered to be the most important model of such the random search, which is a special random walk where each step length is chosen from a power-low distribution with heavy tail (so called Lévy distribution) [44,45]. Therefore, LW shows all scale step length l such that $P(l) \sim l^{\mu}$ with $1 < \mu < 3$, where μ represents the power-low exponent. In the foraging simulations, if prey is abundant and thus probably predictable, it is known that classical random walks such as Brownian motion can yield higher encounter rate than LW. On the other hand, against sparsely and unpredictable located prey, LW is more efficiently than classical random walks.

In this sense, LW has reliable theoretical advantage, yet how about the consistency with empirical data? Indeed, it is reported that among diverse organisms experimental evidences of LW are found [44,46,47]. Of all organisms compared with LW the most noticeable is wandering albatross. In first pioneering work of Viswanathan et al., albatross behavior was followed by a humidity sensor attached to one of its legs [48]. Flight-time intervals were measured by wet periods, and dry points were considered to be landings on the water to catch the fishes. Following research reinvestigating by means of GPS, however, showed that all most long flights were in fact rest time the bird was in its nest, and concluded that the power-low distributed step length is absent in wandering albatross [49]. Though, the latest study which used same method above but examined birds one by one, probed that individuals foraging at sparsely feeder exhibited certain Lévy movement pattern, eventually [50].

A trajectory of LW describes a search pattern composed of many small step clusters interspersed by longer relocations also known as “saltation” [51]. This pattern is provided simple intuitively description using intermittent random search strategy in which slow motion to detect the target is discretely separated from the motion to migrate to another feeder [52]. For example, if we lost a tinny object (e.g. a key) in a huge field (e.g. a beach), we first can consider two simple ways to detect the key. These are slowly careful search and roughly fast one. On the former one, we can make correctly search, but would spend very long time in the beach. On the latter one, we may detect the key speedy, but in many cases its lack of accuracy would result in long search time as same as former one. This is nothing but a trade-off between the exploitation of old certainties and the exploration of new possibilities frequently found in biology [53]. Eventually, to balance this dilemma we would choice the combined one, i.e., intermittent strategy.

In the study of intermittent strategy, it becomes a problem what optimal way to switch the deferent two motions is. Lévy strategy also plays an important role. Bartumeus and his colleague compared correlated random walk (CRW) [54], which is known as a natural way to model the emergence of angular correlations in animal trajectories coming from local scanning, with an intermittent model that is based on CRW but incorporated uncorrelated reorientations with time interval whose length is chosen from Lévy distribution [55]. Then, they showed higher efficiency of this Lévy

intermittent model than non-intermittent one.

Through these theoretical and empirical researches, Lévy strategy has been considered as a key to understand a way of animal search behavior. Consequently, it has been proposed that Lévy strategy has must be strong target for natural selection, so called Lévy foraging hypothesis [43]. Yet, some researchers claim that Lévy-like distribution shown by animals is not necessarily produced by Lévy process. Indeed, few models in which agent walks deterministically and interacts with complex distributed targets, can show LW pattern [56]. Moreover Benhamou, in his confrontational study, suggested by means of combined exponential distributions that there is no guarantee that Lévy-like distribution is based on Lévy process [57].

Here, we will show a simple intermittent model that is not incorporated with Lévy distribution but equipped with principal features of intermittent strategy, i.e., different two phases. In this model, the number of crossovers in a trajectory is regarded as the extent to which agent implements local search and also as a threshold to switch two phases. We demonstrate how this model can balance a trade-off between macro search (exploration) and micro one (exploitation), comparing with CRW. Finally we show that another intermittent search model that is incorporated with an ambiguity with respect to a rule to switch two phases. Such the ambiguity results from a stochastically generated long trail and a search in which agent spends too much times. Moreover, We demonstrate that our model can exhibit efficiency comparable to that of a CRW in an environment with low prey density. By investigating the distribution of switching time intervals, we show that the agent can change foraging strategy depending on prey density. Finally, we discuss how the Lévy distribution can emerge from our model.

4.2. Materials and Methods

4.2.1. Basic Model

First, we present a simple model incorporate main factor of intermittent search in which agent iterate to form local scanning behavior (here we call this exploitation phase) interspersed by longer relocation or saltations (exploration phase) in continuous space and discrete time. Now we call this model EERW in short.

In exploitation phase, agent basically moves as CRW. Here angular correlations are introduced on the basis of circular Gaussian distribution ($-1.0 \leq g \leq 1.0$) centered at the value $g = 0$ (maximum probability), although other distributions (e.g. wrapped Cauchy distribution) might be as good [57]. Turning angle is represented by $\theta = g\pi$. At each step, angle of agent is decided by coupling turning angle with previous angle. Standard deviation (*SD*) of Gaussian distribution controls directional persistence or correlation length of the random walk [60,72].

In intermittent models, agent should migrate to another feeder if local scanning is sufficiently finished. Hence, in EERW, the number of crossovers in a trajectory is regarded as the extent to which agent has searched neighbor area, although switching two phases has usually been implemented by means of stochastic process such as Lévy distribution in previous models [57]. In other words, agent memorizes its trajectory and counts the number of crossovers in the trajectory. A threshold of the number of crossovers to switch two phases is represented by *NC*. Note that *NC* can be estimated

sufficiently as the extent of local search as we discuss later. If the number exceeds a threshold *NC*, the agent makes ballistic movement in the direction uncorrelated to the past, i.e., turning angle is chosen from a uniform distribution $\theta \in [-\pi, \pi]$. Ballistic movement is continued until time-steps that are proportional to the steps spent in exploitation phase. Because the longer time agent spent in exploitation phase, the larger area it would searches, agent should make enough length movement matched with the time spent locally search as relocation. Proportional constant is represented by *P*. And then, because of its finite capacity of memory, agent resets the memory of trajectories, returns to exploitation phase and restarts to walk as CRW at relocated place.

The parameters in our model are listed below:

SD: standard deviation of Gaussian distribution with respect to directional persistency

NC: threshold value of crossover in a trajectory

P: proportional constant with respect to distance in exploration phase

l: step length

In this paper, we fixed the parameter at $l = 0.5$.

Fig. 17a shows the procedure of from exploitation phase to exploration phase. In this case, agent implements exploitation phase as CRW, crossing trajectory three times, i.e., $NC = 3$. Then it transit to exploration phase, making ballistic movement composed of three steps, so *P* is about 0.33 here because the steps is spent nine times at exploitation phase.

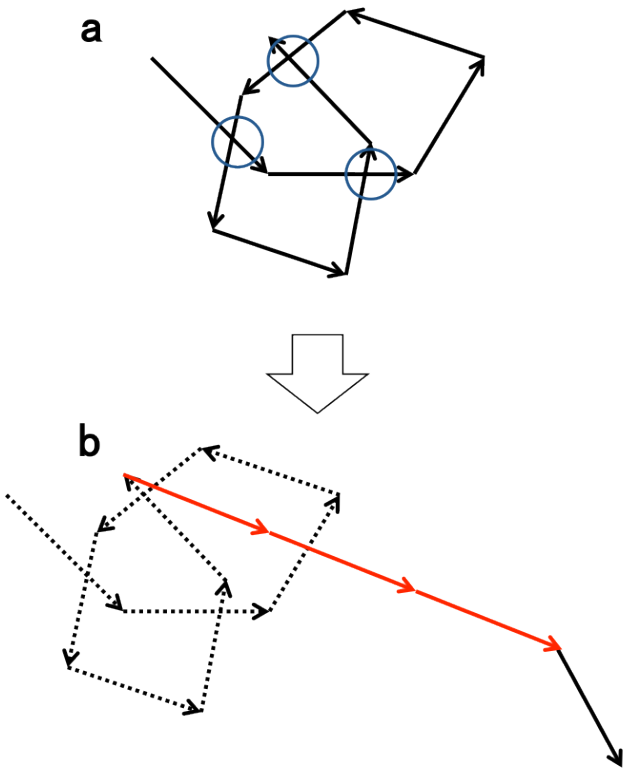

Figure 17. Schematic diagram of phase transition of EERW: (a) Steps of Exploitation phase are represented by black arrows and crossovers are surrounded by blue circles. (b) Steps of Exploration phase are represented by red arrows, and steps of previous and following Exploitation phase are represented by dashed and solid black arrows respectively.

Fig. 18 shows a series of snapshots of total trajectories of CRW and EERW at T = 1000-100000 with SD = 0.3 and l = 0.5, NC =10 and P = 0.3. These simulations are implemented in continuous 2D space with no boundary condition, but are displayed as if it were in space of 200×200 with wrapped boundary condition in Fig. 18. It is easy to see that search area of EERW is broader than one of CRW in spite of same search steps. In many cases, agent imposed search tasks has perceptual range with certain radius, in which agent can detect a target [43]. Then the search efficiency is estimated by number of targets captured in this range. Hence we may partially regard the search areas as alternative for search efficiency. However, if the search area were the most important factor in random search, it holds a strange result such that ballistic movement would become the most optimal strategy. In the next section, we show that EERW can balance a trade-off between macro search (exploration) and micro one (exploitation), which is shown by CRW.

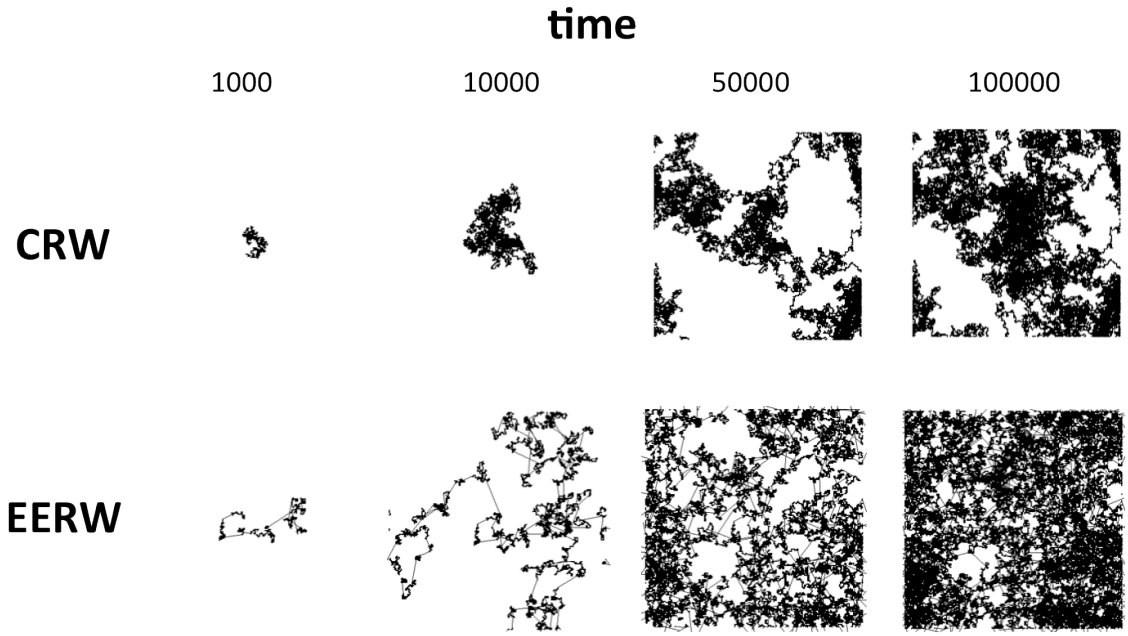

Figure 18. Snapshot of time development of trajectories of CRW (upper side) and EERW (lower side) in a continuous two-dimensional space of 200×200 with wrapped boundary condition. Time proceed from left to right. For both simulations, SD = 0.3 and l = 0.5, and for EERW, NC =10 and P = 0.3. While trajectory of CRW concentrates and overlaps at center of the field, that of EERW sparsely distributes but covers over the field.

4.3. Results

4.3.1. A Trade-off between Macro Search and Micro One

Biological systems, from unit organism to collective animals, are exposed to the trade-off between exploitation and exploration in various levels. Especially the trade-off in open environments biology is dilemmatic decision making of biological systems whether they stay old well-known

environment or they explore new possible environment [52-53,73]. In the case of random (intermittent) search, agent would move to another field if local search were implemented enough. Therefore the exploitation-exploration dilemma would correspond to the relation between micro and macro search. In fact, as mentioned above, if agent moves by means of a strategy leaning to micro search, it would spend long search time in a huge field. Moreover, even if agent detects some targets, there cannot be the most abundant resource. On the other hand, if agent moves by means of a strategy leaning to macro search, it also spends long time to detect targets due to its lack of correctness. Hence, there is a dilemma between micro search and macro one.

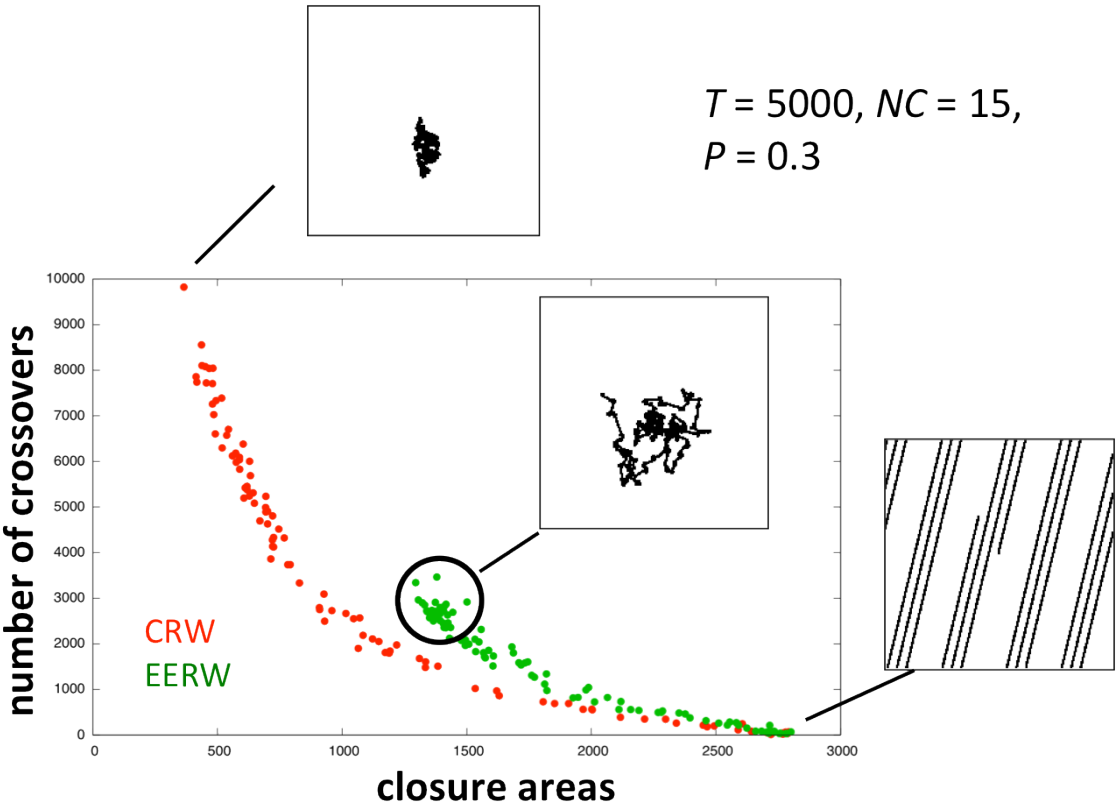

Figure 19. Performance of the CRW (red points) compared with EERW (green points) with respect to the closure areas and the number of crossovers. Snapshots of trajectories of CRW when *SD* is 0.0 and 1.0 are represented by top box and bottom box, respectively. Also that of EERW when *SD* is 0.5 is represented by box connected to black circle, which indicates EERW can balance the trade-off.

In this sense, classical random walk is the most biased strategy against micro search, while ballistic movement is that against macro search. Now, we show that CRW displays micro-macro search trade-off, because if the parameter *SD* approaches zero, behavior of CRW gets closer to ballistic movement, on the other hand, the larger *SD* is, the closer behavior gets to classical random walk. Here, we estimate the extent to which agent implements micro search by means of the number of total crossovers in a trajectory of 5000 time steps simulation, and the extent to which agent implements

macro search by means of closure areas. The closure areas are measured by total neighborhoods areas with radii r = 1.0 where each arrival point of agent is centered. Overall, the trade-off between the micro search represented by the total number of crossovers and the macro search represented by the closure areas is easy to see in Fig. 19, in which patterns of CRW are generated with no boundary condition as varying the parameter *SD* from 0.01 to 1.0 in increments of 0.01. By comparing the patterns of CRW with those of EERW, EERW can balance exploitation with exploration, in which the patterns of EERW are generated under the same conditions as that for CRW except that NC=15 and P=0.3.

Bartumeus and colleague showed that Lévy intermittent model could display higher efficiently than CRW [55]. In their study, Lévy intermittent model were compared with CRW with two deferent values of parameter that controls directional persistency of the model. However CRW can display various behaviors from ballistic movement as extremely directional persistent move to classical random walk as extremely uncorrelated move. Here we examined CRW with all most possible *SD*, revealing that EERW that is the intermittent model without Lévy process can balance trade-off of CRW between exploitation and exploration calculated by two quantities, i.e., closure areas and number of crossovers.

4.3.2. Another Intermittent Search Model

In the study of random search, some models have supposed the presence of memory or learning skills of agent [74,75]. These memory and learning capability also are restricted to be finite. Yet, there is no attempt to assume ambiguity of memory or misunderstanding of learning. In this section, we first introduce ambiguity and/or misunderstanding with respect to a rule to switch two search phases into EERW. Second, we show that such a modified EERW (MEERW, in short) results in Lévy-like distribution of time interval to switch two phases. Finally, we discuss the difference between LW and MEERW.

In EERW, the number of crossovers in a trajectory was regarded as the extent to which agent implements local search. Hence, there was a rule in which if the number exceeds the threshold *NS,* agent switched the phases. On the other hand, in MEERW, though basically same as EERW (Fig.20a), the value of threshold *NS* is dynamically varied by two kinds of misunderstanding of the rule.

As one of such misunderstandings, if a long trail is stochastically generated without enough crossovers, we regarded it as a ballistic movement (Fig. 20b). In the other words, if such the long trail is generated, it is considered that exploitation phase were already implemented even though the number of crossovers did not exceed the threshold *NS*, and exploration phase is regarded as such the trail, entailing reset of the memory of trajectory. Then, *NS* is decremented by one, because agent misunderstands such a shorter local search (and generated trail) as a rule. We here define such a long trail as a series of tracks composed of over N_t tracks, in which inner product of each track and next one is larger than *IP*.

As the other, we introduce further memory restriction, i.e., agent can memorize only N_m number of tracks as trajectory, so can make crossovers only with memorizing tracks (Fig. 20c). Moreover, if agent spends N_s steps without switching two phases, then *NS* is incremented by one, because agent misunderstands such a longer local search as a rule.

In this section, we fixed the parameters at N_t = 15, *IP* = 0.85, N_m = 10, N_s= 100.

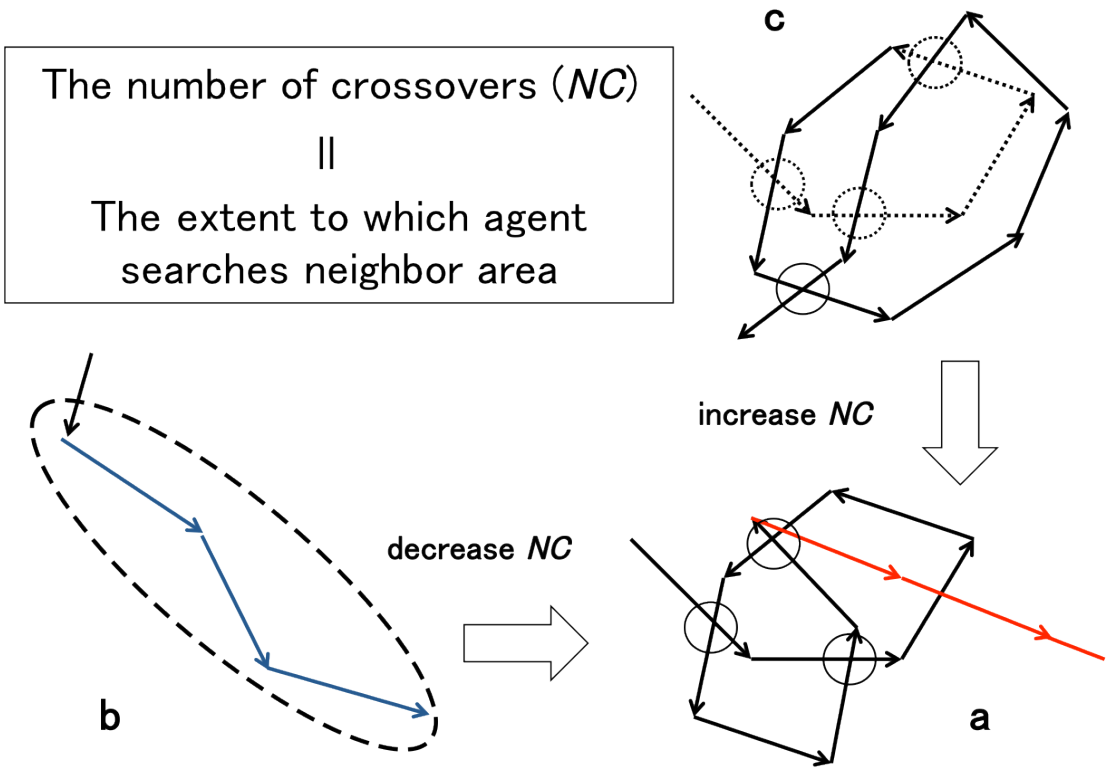

Figure 20. Schematic diagram of MEERW. (a) MEERW is basically same as EERW where *NC* means how long agent searches local area. (b) A long trail stochastically generated decreases *NC*. (c) A search overspent times increases *NC*.

Now, we demonstrate the Lévy-like distribution of time interval to switch two phases, comparing EERW and MEERW. For EERW, we measured the time steps spent in the exploitation phase as the time interval because the proportion of time steps spent in the exploitation phase to that in the exploration phase is constant. For MEERW, basically we measure time steps by same manner for EERW, but if the stochastic long trail is generated, we also measure time steps from start of exploitation phase until this trail is generated. Fig. 21 shows frequency distributions of time interval which is observed in one million time steps simulation with $SD = 0.2$ and $P = 0.3$. The exponent μ is computed by a slope of a regression line for the range of values where power law behavior (straight line in a log-log plot) is observable. The exponent μ of EERW is 5.81 with $R^2 = 0.957$, while that of MEERW is 2.38 with $R^2 = 0.943$.

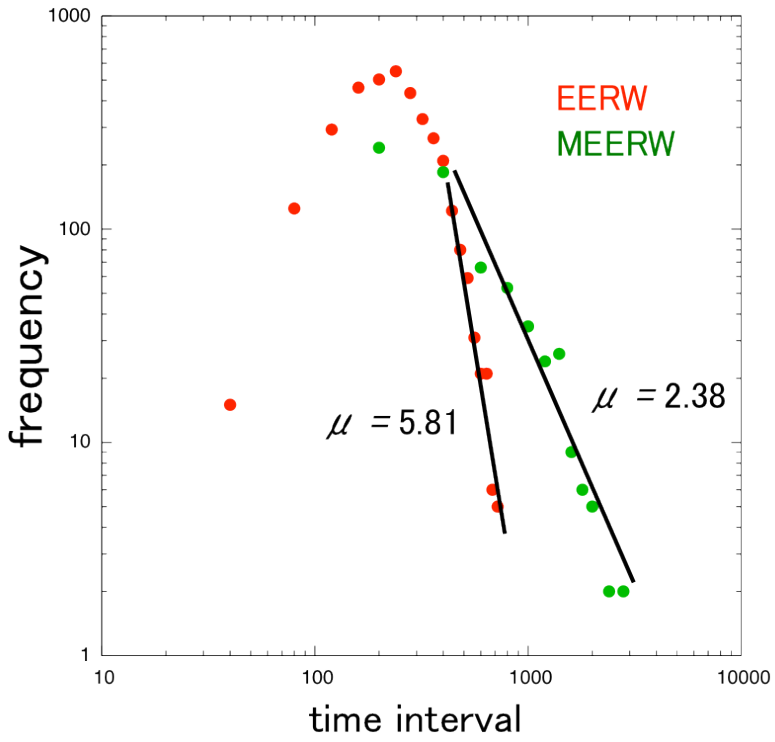

Figure 21. Power law distributions of EERW and MEERW.

In the Lévy strategy, also including the Lévy intermittent model, the exponent μ of the tail of power law distribution should lie in the interval $1 < \mu < 3$. For $1 \geq \mu$, the distribution is not defined. For $\mu \geq 3$, provided the conditions of the Generalized Central Limit Theorem, the tail converges to a Gaussian distribution. In the latter case, the time interval will show an intrinsic characteristic scale. In this sense, distribution of MEERW is considered to be Lévy-type, but that of EERW is not.

		NC=1	*NC*=10	*NC*=20
SD=0.1	μ	5.472	5.066	4.602
	R^2	0.95724	0.92954	0.90619
SD=0.5	μ	6.465	6.303	8.426
	R^2	0.9613	0.95194	0.93657
SD=0.9	μ	7.771	9.071	7.691
	R^2	0.94909	0.95885	0.93114

Table 6. Estimation of the exponent μ of EERW with the parameters *NC* and *SD*.

Indeed, the distribution of EERW cannot be Lévy-type. In table 6, we estimated the exponent μ of EERW, varying the parameter *NC* from 1 to 20 and *SD* from 0.1 to 0.9. The result shows that at all combinations of *NC* and *SD*, the exponent μ is bigger than 3 with high correlation ($R^2 > 0.9$). What is the difference between LW and MEERW? It is hard to distinguish the both LW and MEERW, when we set the step length l as very small against the parameter P (Fig. 22).

Figure 22. Snapshot of a trajectory of MEERW with l =0.005 and P = 3.0.

4.3.3. Search strategies depending on prey density

In this section, we investigate the prey-detecting efficiency of our model with P=0.4 and l=0.1 in two environmental contexts - low and high prey density - compared to a CRW. Furthermore, by examining the distribution of switching time intervals, we show how agents in our model can change foraging strategy depending on prey density.

To examine the behavior's dependence on prey density, we used a simple search scenario where prey is located at each vertex of a lattice in a 2D, continuous, 400×400 space with wrapped boundary conditions. The prey density λ is defined by the side length of the lattice; we set λ=3 for high density and λ=10 for low density. The detection range is defined as twice the step length, *i.e.*, the agent can detect the target if the distance between the agent and target is less than 2l (Figure 23). After the agent detects the target, reorientation takes place as in [55], *i.e.*, the agent chooses its next turning angle from a uniform distribution in both our model and the CRW, and the agent in our model restarts the exploitation phase, resetting the number of crossovers to zero.

We first examine the behavior of our model in different environments with non-destructive search to maintain a uniform density condition. Figure 24a,b show snapshots of trajectories in the high- and low-density conditions, respectively. It is easy to see that the agent can implement a smaller range of saltation lengths in the lower density condition compared to the higher density condition. This results from refreshing the number of crossovers, *i.e.*, in the higher density condition, because the agent frequently contacts prey, the misunderstanding of the rule to switch phases can only rarely occur; therefore, the threshold *NC* tends to be fixed. On the other hand, in the higher density condition, the

agent rarely contacts prey and can move more freely. Therefore, the misunderstanding is implemented, and a greater variety of search times in the exploitation phase and of saltation lengths is observed (see later in this section for a more detailed discussion).

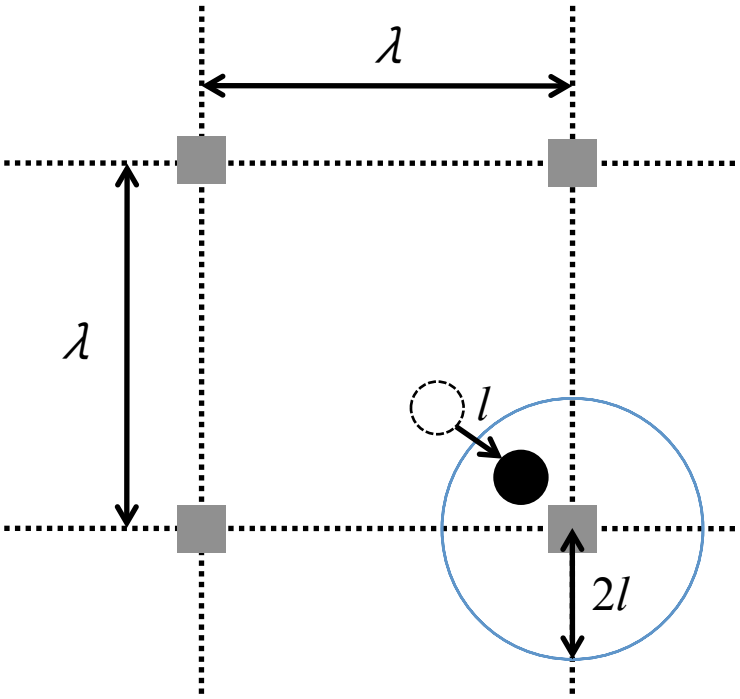

Figure 23. Schematic diagram of detecting behavior in our model. Target prey represented by grey squares is arranged with spacing λ on a continuous, two-dimensional space of size 400×400 with wrapped boundary conditions. The agent moves from the previous location (dashed circle) to the present location (black full circle) with step length l. If the agent enters the perception range with radius of $2l$, represented by a blue circle, it can capture the prey.

Next, we examine the distributions of time intervals for phase switching (which is also proportional to the saltation length) in the low- and high-density condition (Figure 24c,d). The distribution in the low-density case displays a power-law decay (power-law versus exponential [49], N=44, μ=2.45, λ=0.0023, w_p= 0.93, w_{exp} = 0.07), whereas the distribution in the high-density case displays an exponential decay (power-law versus exponential, N=44, μ=2.43, λ=0.0063, w_p= 0.0, w_{exp} = 1.0). In the Lévy strategy with the Lévy intermittent model, the exponent μ of the power-law distribution should be in the interval $1 < \mu < 3$. For $\mu \leq 1$, the distribution is not defined. For $\mu \geq 3$, provided the conditions of the Generalized Central Limit Theorem, the tail converges to a Gaussian distribution. In the latter case, the time interval will show an intrinsic characteristic scale. In this sense, the distribution in the low-density case is Lévy but that in high-density case is Brownian. Furthermore, we estimate the search efficiency both in low- and high-density environment with destructive conditions, compared to the CRW model. We ran 30 trials in a limited period of 30 000 time steps. Figure 25a,b show the performance of both our model and the CRW at high- and low-density, respectively. In low-density condition, the number of captured prey for our model is significantly larger than for the

CRW (*t*-test, $p < 10^{-5}$). On the other hand, there is no significant difference in the number of captured prey between our model and the CRW in the high-density condition (*t*-test, $p = 0.485$, n.s.). It could be concluded that in this case, because of its Brownian-type saltation, the behavior of our model is little different than CRW. However, when the agent searches for a longer time (60 000 and 90 000 time steps), our model captures significantly more prey than the CRW (T=60 000: *t*-test, $p = 0.0022$; T=90 000: *t*-test, $p < 10^{-8}$) (Figure 25c). The longer the agent searches, the fewer prey remain. Thus, prey density gradually decreases, which would create conditions allowing misunderstanding of the rule.

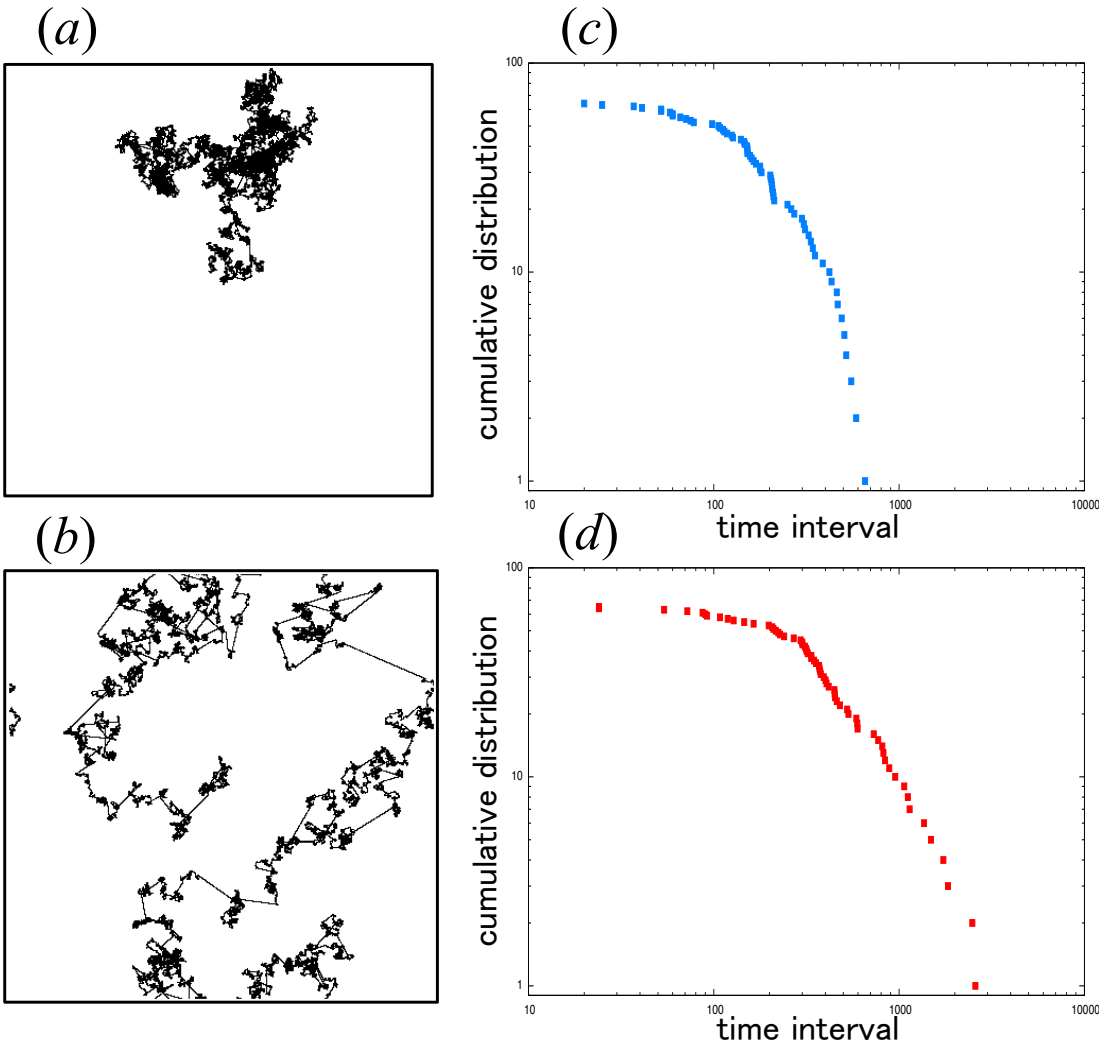

Figure 24. Autonomous change of behavior depending on environmental context. (*a*) Snapshot of the trajectories after 300 000 time steps in the higher density condition ($\lambda = 3$) (*b*) Snapshot of the trajectories after 300 000 time steps in the lower density condition ($\lambda = 10$). (*c*) Log-log plot of the distribution of time intervals for phase switching at higher density. (*d*) Log-log plot of the distribution of time intervals for phase switching at lower density.

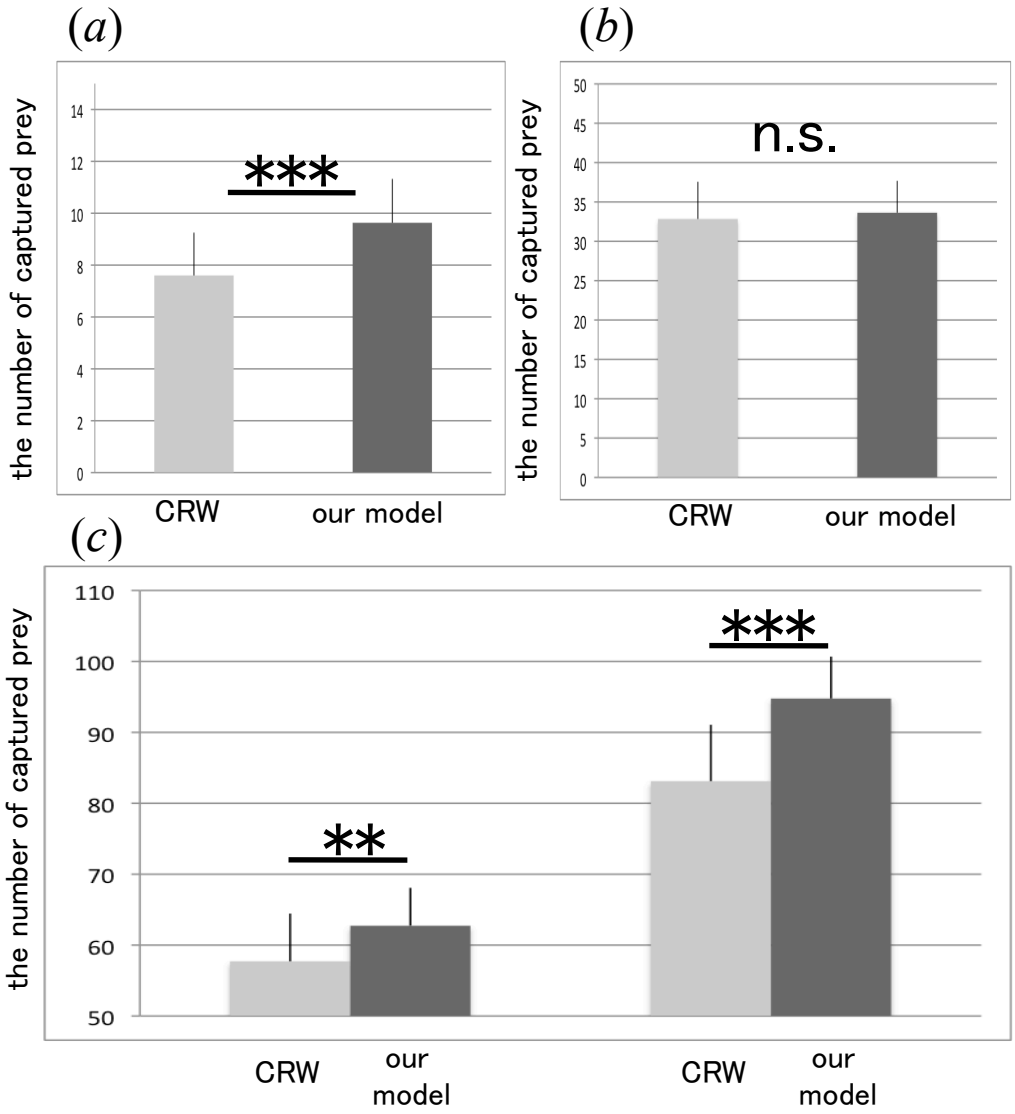

Figure 25. The search efficiency of the CRW (pale grey bar) and our model (dark grey bar) with respect to search efficiency. (*a*) The lower density case. The vertical axis represents the mean value for 30 trials of the number of captured prey during 30 000 time steps. (*b*) As in A, for the higher density case. (*c*) A longer search time at higher density with T = 60 000 (left) and 90 000 (right). Error bars are standard deviations. ** $p < 0.01$, *** $p < 0.001$, n.s. indicates not significant.

Furthermore, to investigate how the degree of *NC* change relates to prey density, we set a smaller space (100×100) and higher density (λ=2) with destructive conditions and ran one million time steps. Figure 26 shows the normalized change of *NC* at each time interval, with bin size T'=100 000 (Δ*NC*), and the proportion of remaining prey (*R*) at each time step versus time step. Note that the change in *NC* at each bin Δ*NC* is defined by $\Sigma^{T'}_{t'=0} |NC_{t'}-NC_{t'-1}|$, where $NC_{t'}$ represents *NC* at each time step, and this is normalized such that max(Δ*NC*) = 1.0. It is easy to see that the smaller *R*, the greater Δ*NC* is, indicating that the agent uses a greater variety of search strategies at low-density than at

high-density.

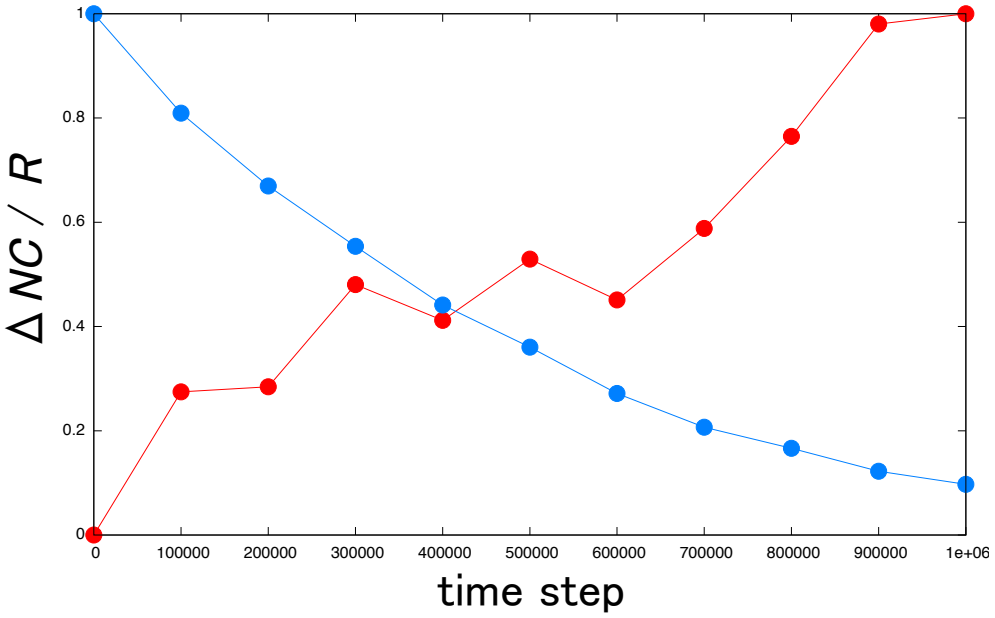

Figure 26. The relationship between the prey density and the change in *NC*. Δ*NC* (red points) and *R* (blue points) are plotted against time step, where Δ*NC* represents the normalized change in *NC* at each time interval with bin size *T'*=100 000, and *R* represents the percentage of prey remaining .

These results indicate that our model can efficiently change search strategy from Brownian-type to Lévy-type depending on the prey density. In the next section, we discuss how the Lévy distribution can emerge from our model.

4.3.4. Lévy distribution without Lévy process

The Lévy strategy has been established as a key to understand animal search behavior using both theoretical and empirical studies. Consequently, it has been proposed that the Lévy strategy must be a strong target for natural selection. This is the so-called Lévy foraging hypothesis (Viswanathan et al., 2011). Still, some researchers claim that the Lévy distribution exhibited by animals is not necessarily produced by a Lévy process. Indeed, few models in which an agent walks deterministically and interacts with complex distributed targets can show an LW pattern [56]. Moreover, Benhamou used a composition of exponential distributions to suggest that there is no guarantee that the Lévy distribution exhibited by an animal is based on a Lévy process [57].

In the case of our model, the Lévy distribution appears to arise from a superposition of several distributions caused by a varying value of *NC*, similar to a Cox process, which is a mixed Poisson process. It is known that the Cox process can generate heavy-tailed and power-law distributions [79]. We previously showed that if *NC* is fixed to a certain value, the time intervals do not exhibit a Lévy-type distribution, which is similar to the high-density prey condition described above. Therefore, to determine whether such a mixed distribution creates the Lévy distribution in our model, we

investigated whether the Lévy distribution can emerge when we forcibly rearrange the value of *NC* in descending order. First, we obtained distributions of time intervals for phase switching in a field with no prey (power-law versus exponential, N=38, μ=2.43, λ=0.0019, w_p= 0.94, w_{exp} = 0.06) (Figure 27a), checking the value of *NC* at each time step. At this time, because *NC* is not related to the agent's behavior in exploration phase, we set P = 0.0, *i.e.*, there is only an exploitation phase. Figure 27b shows the ratio of *NC* at each time step. When we forcibly rearranged the value of *NC* in descending order, we could observe a Lévy distribution (power-law versus exponential, N=43, μ=2.39, λ=0.0018, w_p= 0.92, w_{exp} = 0.08) (Figure 27c). In Figure 27d, a distribution with *NC*=1 is shown, which is clearly distinguishable from that for *NC*≠1. It is clear that the tail part of the original distribution matches the distribution with *NC*≠1, and the rest of the original distribution matches that with *NC*=1.

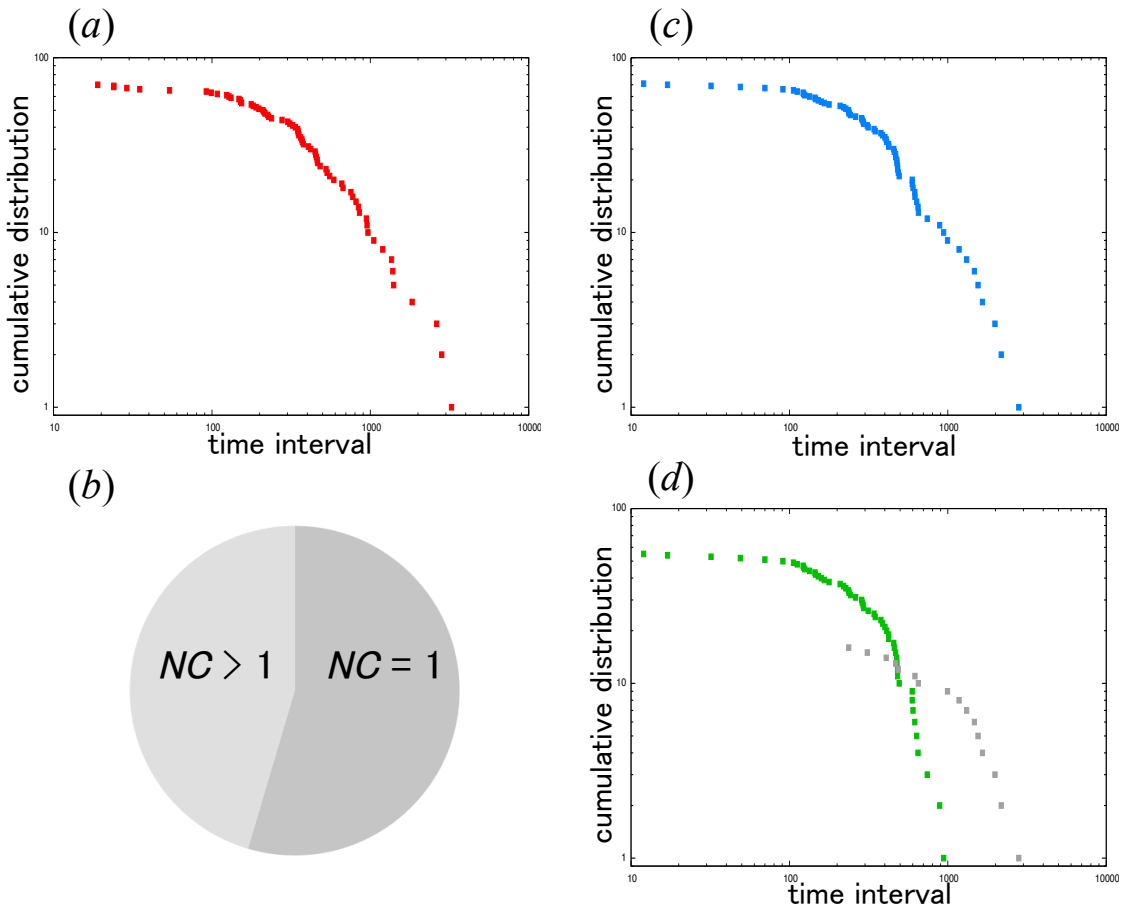

Figure 27. Lévy distribution as a mixed distribution. (*a*) Log-log plot of the distribution of time intervals for phase switching without prey. Because *NC* is not related to the agent's behavior in the exploration phase, we set P = 0.0. (*b*) The ratio of the distribution for *NC* = 1 to that for the simulation in Figure 27a. (*c*) Log-log plot of the distribution with the values of *NC* obtained by the simulation in Figure 27a forcibly rearranged in descending order. (*d*) Log-log plot of the distribution for *NC* =1 (green points), distinguishing it from that for *NC*>1 (pale grey points).

4.4. Discussion

The Phenomenon that local clusters are connected by the saltations in animal search and/or LW, suggests that there are some sort of rules with respect to detection for targets [52]). The intermittent search strategy explain that agent to have a rule that agent move to another field if local search were implemented enough, so as to be consistent with this phenomenon. Then agent has two deferent phases. However, time interval to switch two phases has eventually been given by some stochastic process such as Lévy process rather than a rule.

In this chapter, we started with the simple intermittent model EERW that was not incorporated with Lévy process but equipped with principal features of intermittent strategy (i.e., different two phases). In EERW, the switch of two phases is provided as a rule that if the number of crossovers exceeds a threshold *NC*, the agent resets the memory of trajectories and makes ballistic long trails in the direction uncorrelated to the past. We demonstrated that EERW could balance a trade-off between macro search (exploration) and micro one (exploitation), comparing with CRW.

We constructed MEERW by incorporating ambiguity or misunderstanding of the rule, in which a threshold *NC* is dynamically varied by the stochastically generated long trail and the search spent too much times. As a result, MEERW showed Lévy-like distribution. Moreover, depending on the parameter *l* and *P*, MEERW could behave as if it were just LW.

Already LW has been constructed without Lévy process, yet there must have been deterministic walks and interactions with complex distribution of targets [56]. So our model is the first attempt to investigate hypothesis that LW can be generated with the absence of Lévy process as well as of deterministic walks.

While optimal change of search strategy has long been predicted [77], empirical evidence has only recently been reported. This evidence of a change in strategy depending on environmental context implies that animal movement does not obey one single distribution. In this paper, we began with a simple model that possesses the principal features of an intermittent strategy, *i.e.*, careful local searches separated by longer steps or saltations, such as relocation, where the agent follows a rule to switch between the two phases, but it could misunderstand this rule, *i.e.*, the agent follows an ambiguous switching rule.

This ambiguity of the rule gives rise to continual changes in the agent's foraging strategy. We showed that an agent of our model can exhibit different types of search strategies depending on environmental context, changing from Brownian-type in high-density conditions to Lévy-type in low-density conditions. Furthermore, our model can exhibit higher efficiency than a CRW in both environmental contexts. In this way, the change in foraging strategy of our model agrees with recent empirical results [78]. The most important point is that depending on prey density, the agent can change its foraging strategy autonomously without any concrete information with respect to environmental state. All that is required is the condition that if the agent makes contact with prey, then it refreshes its state and restarts its search.

Moreover, we investigated the relationship between prey density and the change in *NC*, where *NC* is the extent to which the agent has searched the surrounding area. As a result, we observed that the lower the prey density, the greater the change in *NC*. This implies that while many changes of strategy

occur in the scarce resources environment, the agent tends to fix its strategy in an abundant environment. In the previous section, we illustrated how the Lévy distribution in our model emerges without a Lévy process. Such a Lévy distribution without a Lévy process has already been constructed, but this required deterministic walks and interactions with a complex distribution of targets [56], as well as the assumption that the agent must have information of target locations, no matter how great the distance between the agent and a target. On the other hand, an agent in our model has neither this information nor a Lévy process. Instead, our model generates a Lévy distribution by composing the various distributions arising from different values of *NC*, as seen in Figure 27d.

The fact that local clusters are connected by saltations in animal searches suggests that there are rules for the detection of targets [52]. Our model is the first attempt to introduce ambiguity in the rule for switching between such saltations and the small steps characterizing local exploitation. In this way, an agent in our model can adopt a flexible search strategy. Therefore, this model may provide key insight into how animals can flexibly respond to the environment.

5. Collective Animal Foraging Driven by Inherent Noise

5.1 Background

In study of collective behavior, both escapes from predatory attacks and collective foraging against surroundings of animal groups are mainly considered as collective response to external environment. Recently the former has been investigated in detail by using starling flocks [e.g., 17,58]. For example, density wave within the flock, which can transfer information derived from external perturbation (e.g. predations by falcons) faster than their flight speed, is found [58]. On the other hand, although the latter is referred in introduction of many papers regarding collective behavior, related experiment is rare.

We here conducted an experiment with respect to collective foraging behavior of a swarm of soldier crabs *Mictyris guinotae*, which live in the tideland and can form large swarms. We collected them in two hours before ebb tide and conveyed to the laboratory. By using markers attached to crabs' shells and image-processing software, we obtained time series of individuals' position during thirty minutes.

To investigate the behavior, we created two experimental apparatus: ring- and round-shaped arenas. First, we checked basic behavior of soldier crab swarm in the round-shaped arena. Next, to examine characteristics of the behavior, and to simplify analysis, we used the ring-shaped arena. In the ring-shaped arena, the behavior of crabs would be regarded to be approximately one-dimensional.

Buhl et al. [10] conducted an experiment with respect to one-dimensional behavior of aggregating locusts in the ring-shaped arena, and observed that phase transition from disordered state to ordered state with respect to direction of locusts is dependent on this density. In their experiment, they simply considered "*swarm"* to be an aggregation of locusts that distributed in the arena. On the other hand, we here investigated whether soldier crabs formed denser swarm on the inside of the arena, and whether they showed collective foraging behavior.

5.2. Materials and Methods

5.2.1. Experimental Setup

Here we used soldier crab *M. guinotae*. We presented a detailed description of this specie in the section 3.2.1, so see further details in the section. Although *M. guinotae* burrows tunnels and lives under substrate at higher tidal levels, they emerge and feed on detritus on the lagoon surface in swarms at the lower tidal level. Through numerous field surveys of soldier crabs, we found that they search and wander on the lagoon surface during the two hours around ebb tide, keeping densely swarm to some extent and feeding on detritus. We collected them in plastic containers that contained mud substrate in two hours before ebb tide on fine weather days in July and August 2014 and conveyed to the laboratory. Our experiment was conducted in the daytime during the 3 hours around ebb tide. For each trial different swarm composed of different crabs were used. All crabs used in a trial were individually

marked with paper triangle prisms on the shell. Crabs were immediately took off the markers and released after the experiment.

5.2.2. Marking

To simplify the tracking of identified individual movement of animal group, marking or tagging have been frequently used methods [8,9].

Immediately before each trial we attached markers, which were shaped in the form of triangle prisms whose side length are 5 mm and were made of thick white paper, on each individual crabs' shells by using gum arabic paste (Fig. 28). After that marked crabs were separated into each size swarm and moved to each experimental arena without pre-training.

Figure 28. Marked crab. Side length of marker, 5mm.

5.2.3. Experimental Arena

We designed two kinds of experimental arenas: ring- and round-shaped arenas (both outside diameters, 120 cm; inside diameter of ring-shaped arena, 60 cm; both heights, 10 cm). Both arenas were composed of plastic cardboards (wall) and styrene board (floor), and covered by black tapes to make a contrast with crabs' white markers. We recorded behaviors of soldier crab swarms with 10, 20, 30, 40 individuals in each experimental arena by using overhead video camera (Panasonic HDC-TM700, 1920 ×1080 pixels).

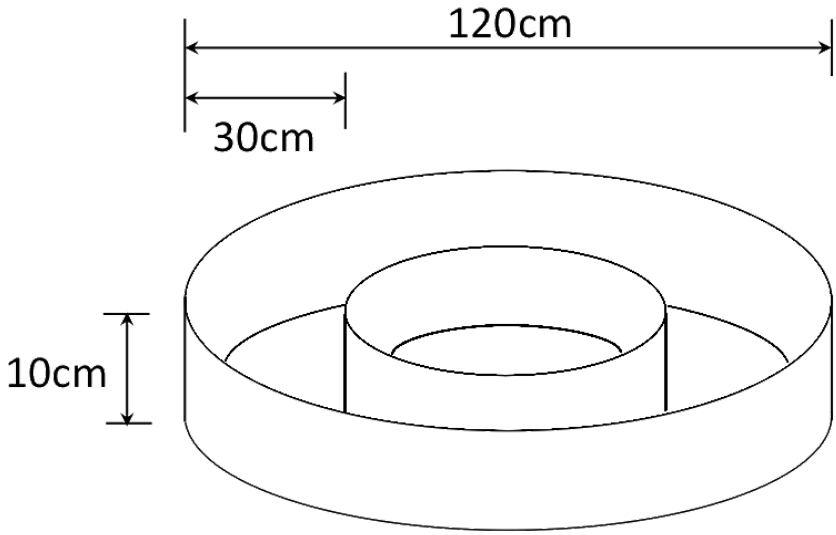

Figure29. Illustration of ring-shaped arena. Round-shaped arena has the same outside diameter and height as ring-shaped one.

5.2.4. Tracking

Time series of identified individuals' positions were tracked using image-processing software (Library Move-tr/2D ver. 8.31; Library Co. Ltd., Tokyo, Japan) in the same manner described in the section 2.2.2. The geometric center of markers of each crabs were identified by the fact that the marker appears lighter than the surrounding area, and the crab trajectories were constructed by tracking individuals from one frame to the next. When crabs fell down and thereby its marker was concealed, we identified its position using the manual-tracking mode of the software. As a result, we obtained all of the individuals' x–y coordinates during thirty minuets. In this study, the time interval between two consecutive reconstructions of individuals' coordinates was dt=0.2 sec.

5.3. Results

5.3.1. Collective Foraging Behavior of Soldier Crab Swarm in the Arena

In the case of behavior of crabs in round-shaped arena, we observed that (i) crabs basically moved around or along the wall of the arena; (ii) the movement of the swarm along the wall was occasionally changed its direction with respect to the center of arena (iii) crabs formed dense swarm to some extent. To observe above behaviors in detail, we here investigate the behavior of the swarm in the ring-shaped arena.

We here show the behavior of soldier crab swarm in the ring-shaped arena. Previous experiment regarding collective behavior in ring-shaped arena revealed that, in aggregating desert locusts, a one-dimensional phase transition from disorder to order occurs, as the density of locusts in the arena increases. In this case, an aggregation of locusts distributed in the arena is considered as a single

group. On the other hand, we here investigated if crabs formed a densely swarm in local area of the arena and that there were some foraging patterns in the behavior of the swarm.

5.3.2. Do Crabs Swarm to What Extent?

To estimate to what extent crabs swarm, we defined an individual position as a radial position with respect to the center of the arena, i.e., we obtained it as one-dimensional position as in the case of locust experiment. In the other words, individual radial position $x_{t,i}$ is defined as one-dimensional coordinate ranging from $0 \leq x_{t,i} < 360$(degree). In the same way, we acquired one-dimensional radial position of the center of the mass of swarm with respect to the center of arena, X_t. Then individual relative position with respect to the center of the mass was calculated as $rx_{t,i} = X_t - x_{t,i}$, where $|rx_{t,i}| > \pi$.

$rx_{t,i}$ may indicates to what extent crab i is far from or near the center of the mass. So if the dispersion of the distribution of $rx_{t,i}$ throughout the trial is small enough, the swarm can be considered to be dense to some extent. When we compared the dispersion of real swarm with control where individuals' positions were randomly distributed in the arena, real one was significantly smaller than control one (Fig. 30) (Bartlett's test; 10 individuals: real (N=90000, variance=1.67) vs control (N=90000, variance=2.22): χ^2_1=1817.3, P<2.2e-16; 20 individuals: real (N=180000, variance=1.73) vs control (N=180000, variance=2.52): χ^2_1=6329.3, P<2.2e-16; 30 individuals: real (N=270000, variance=2.12) vs control (N=270000, variance=2.66): χ^2_1=3468.0, P<2.2e-16; 40 individuals: real (N=720000, variance=2.18) vs control (N=720000, variance=2.75):, χ^2_1=9658.0, P<2.2e-16). Fig. 31 presents the frequency distribution of $rx_{t,i}$.

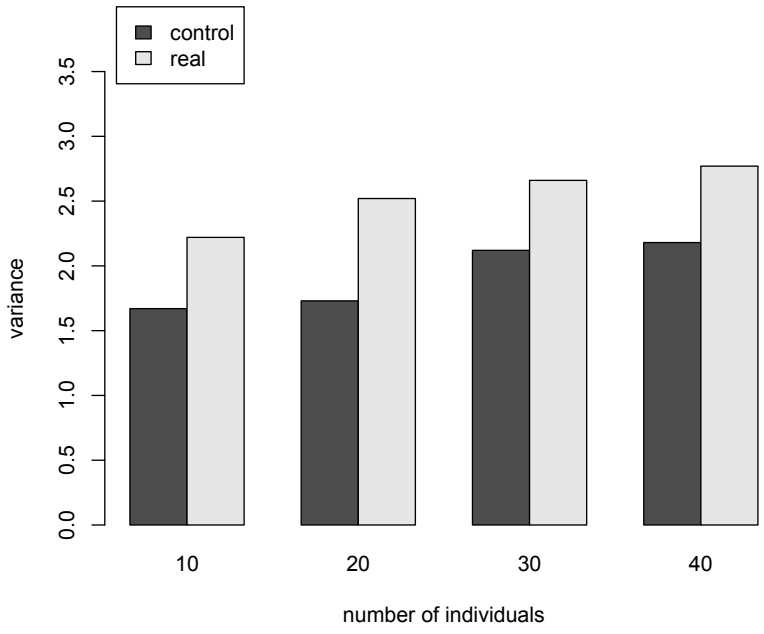

Figure 30. Comparison between the dispersion of real swarms and control where individuals' positions were randomly distributed in the arena.

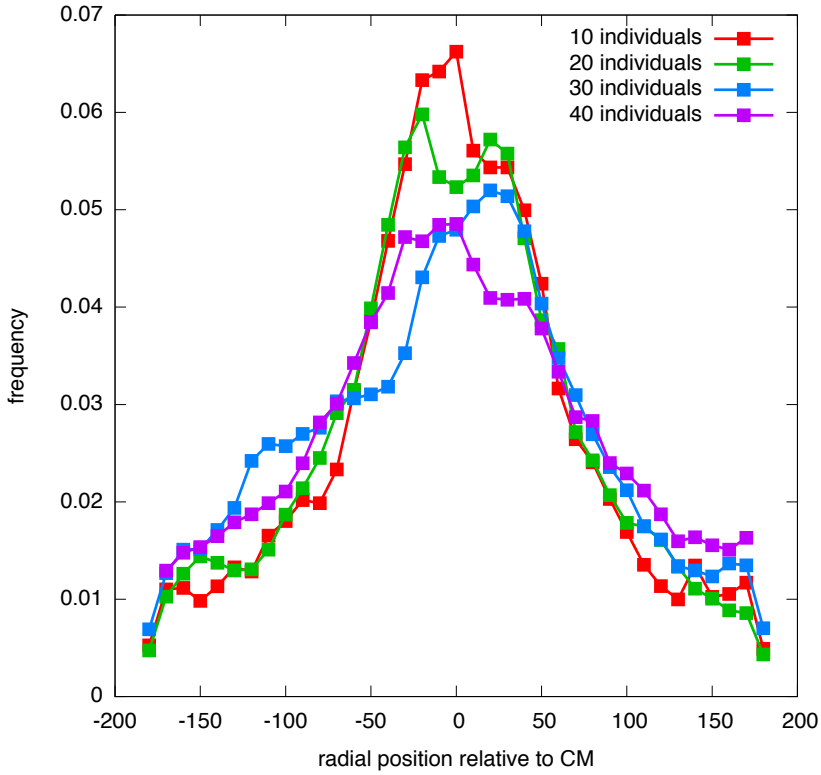

Figure 31. frequency distribution of $rx_{t,i}$.

5.3.3. Durations of Direction Changes of the Center of the Mass of Swarm Show Power-law Distribution

For the swarm discussed above (i.e., swarm that is dense to some extent), investigation of the behavior of the radial position of the center of the mass may be meaningful in investigating of the collective foraging. Fig. 32 shows time transition of radial position of the center of the mass.

We defined the direction change of the center of the mass by examining whether it switched its head direction from clockwise to anticlockwise or vice versa between time steps. When we calculated the time between direction changes, we found that it followed power-law distribution (power-law vs exponential (ref. [49]); 10 individuals: N=313, μ=−1.49, $w(p)$=1.00; 20 individuals: N=157, μ=−1.39, $w(p)$=1.00; 30 individuals: N=174, μ=−1.44, $w(p)$=1.00; 40 individuals: N=237, μ=−1.50, $w(p)$=1.00) (Fig. 33).

5.4. Discussion

In this chapter, with respect to the behavior of soldier crab swarm in the experimental arenas, we found the following observations: (i) the swarm of soldier crabs forms densely swarm to some extent. (ii) We calculated the time between direction changes of the swarm, and found that it followed power-law distribution, containing very long moves (of greater than 100 sec). Such movement pattern is better described by means of Lévy walk than Brownian walk. Indeed, the power-law exponent μ systematically ranges in the interval $1<-\mu\leq 3$, which is a signature of Lévy pattern [44]. For predatory

animals, Lévy pattern is a foraging pattern that balances exploitation and exploration foraging. While there are many movement data of single predatory animals, our result is the first example of Lévy walk exhibited as collective foraging.

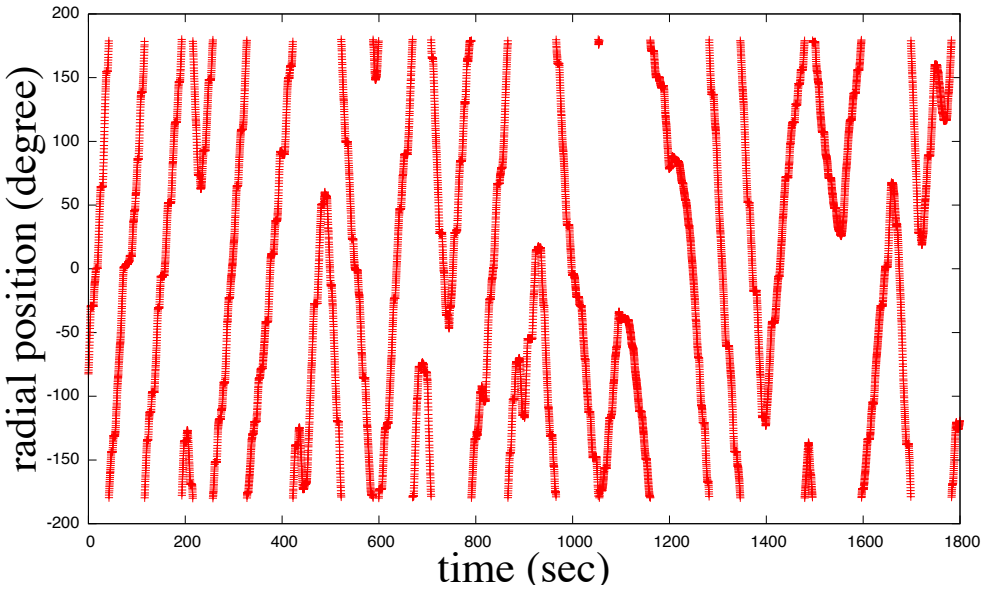

Figure 32. Time transition of radial position of the center of the mass of the swarm with 40 individuals in the ring-shaped arena.

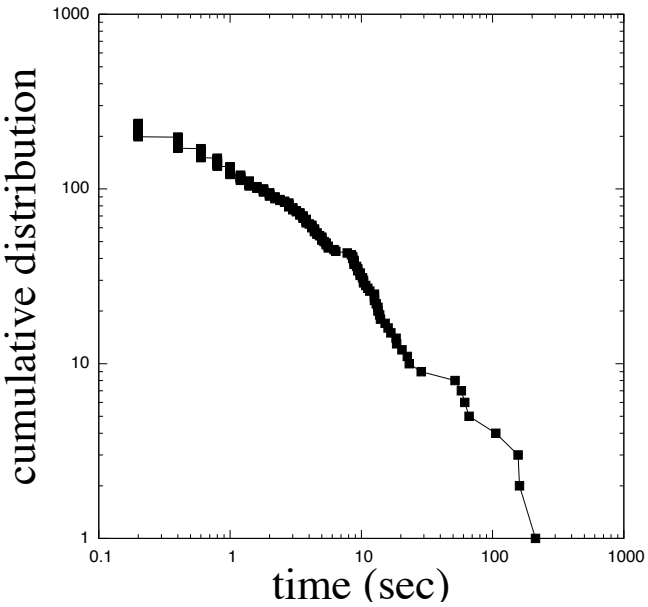

Figure 33. Cumulative distribution of duration between consecutive direction changes of the center of the mass of the swarm with 40 individuals in the ring-shaped arena.

How does the soldier crab swarm carry out this emergent pattern? The swarm of the species has inherent noise that is individuals' different velocities in maintaining a densely and directed swarm. Such an inherent noise has been found not only in the swarming of soldier crabs but also in other animal groups (e.g., [24,26]). Hence, the coexistence between the group as a whole and diversity of individuals' movements may be a common trait of collective animal groups. According to theoretical models [76], animal group can make changes of its direction by making noise. It can be considered that the swarm of soldier crabs realizes the Lévy pattern strategy by taming the inherent noise.

6. Conclusion

In previous simulating study of collective behavior, most important rule to create collectiveness is regarded as "velocity matching" by which individual agent interacts with its neighbors in neighborhood with a fixed radius by averaging the directions of motion of its neighbors. In addition to this rule, "external noise" selected from equal probability with certain magnitude is coupled with agent's velocity, by which agent's movement is added some randomness. In this framework, collective behavior such as one-directional and coherent motion is achieved by velocity matching, having lack individuality. On the contrary, diversity of individual movement is acquired by external noise, neglecting the collectiveness. There is, therefore, an opposed relationship between velocity matching to create collective group and external noise to collapse the group. Recent empirical studies, however, suggest that it is doubtful whether such relationship is in real collective animals. In this thesis, we defined such diverse movements of individuals in coherent group with one-directional movement as "inherent noise".

In chapter 2, we firstly investigated "inherent noise" in schooling ayu fish. Here we showed that noise generated inherently in a school of ayu fish is characterized by various power-law behaviors in contravention of the prediction of previous models. First, we showed that individual fish move faster than Brownian walkers with respect to the center of the mass of the school as a super-diffusive behavior, as seen in starling flocks. Second, we assessed neighbor shuffling by measuring the duration of pair-wise contact and find that this distribution obeys the power law. Finally, we showed that an individual's movement in the center of a mass reference frame displays a Lévy walk pattern. This fact may mean that by inherent noise each individual searches "communication" among other individuals; new communication is explored, and familiar communication among neighbors is exploited. In conclusion, our findings in this chapter suggest that inherent noise (i.e., movements and changes in the relations between neighbors in a directed group) is co-exist with coherent and one-dimensional motion of schooling fish, and is dynamically self-organized in both time and space. In particular, Lévy walk in schools can be regarded as a well-balanced movement to facilitate dynamic collective motion and information transfer throughout the group.

In chapter 3, we presented an emergent behavior driven by inherent noise. Emergent behavior that results from a mass effect is one of the most striking aspects of collective animal groups. Investigating such behavior would be important in order to understand how individuals interact with their neighbors. We showed that a swarm of soldier crabs, *Mictyris guinotae*, could spontaneously enter a water pool, which are usually avoided, by forming densely populated part of a swarm at the edge of the water pool. Moreover, we showed that the observed behavior can be explained by the model of collective behavior based on inherent noise and mutual anticipation. Inherent noise in the model created diverse potentials for each individual. By using the diversity of moves for other individuals' anticipation, a densely collective swarm emerges. In our model, after regions of high concentration are formed, the swarm can enter the pool and make mutual anticipation at sites in the pool due to highly concentrated potential transitions. In conclusion, our results in this chapter suggest that inherent noise can contribute to formation and/or maintenance of a swarm and that the dense swarm can enter the pool by means of enhanced inherent noise.

In the chapter 4, we explained animal foraging strategy through our new foraging model, as an introduction for collective animal foraging shown in the chapter 5. We here began with a simple model that possesses the principal features of an intermittent strategy, *i.e.*, careful local searches separated by longer steps or "saltations", as a mechanism for relocation, where the agent follows a rule to switch between two phases, but it could misunderstand this rule, *i.e.*, the agent follows an ambiguous switching rule. Thanks to this ambiguity, the agent's foraging strategy can continuously change. First, we showed that this model could balance a trade-off between macro search (exploration) and micro one (exploitation), which is shown by CRW. We demonstrated that another intermittent search model that is incorporated with ambiguity with respect to the rule to switch two phases, counld show Lévy-like distribution of the time interval. Next, we demonstrated that our model can exhibit an optimal change of strategy from Brownian-type to Lévy-type depending on the prey density, and we investigated the distribution of time intervals for switching between the phases. Moreover, we shoed the model can display higher search efficiency than a correlated random walk. Finally, we discussed how a Lévy distribution can emerge from our model.

In chapter 5, we investigated whether collective animal foraging behavior is driven by inherent noise. We here conducted an experiment with respect to collective foraging behavior of a swarm of soldier crabs. To investigate the behavior, we mainly used ring-shaped experimental apparatus by which the behavior of crabs would be regarded to be approximately one-dimensional. We here investigated whether soldier crabs formed denser swarm on the inside of the arena, and presented they showed Lévy-like behavior as collective foraging behavior. In conclusion, our results in this chapter suggest that the swarm of soldier crabs realizes the Lévy pattern strategy by taming the inherent noise.

A summary of conclusion of this thesis is as follows. (i) "Inherent noise" is co-exist with coherent and one-dimensional motion of schooling fish, and is used for searching "communication" in collective animal group (chapter 2). (ii) "Inherent noise" can contribute to formation and/or maintenance of a swarm, and make it possible to carry out some kind of emergent behavior (chapter 3), (iii) "Inherent noise" can promote collective foraging behavior such as the Lévy pattern (chapter 4,5). We think that the co-existence between diversity of individuality and collectiveness as a whole, by which collective groups establish the robust system, will be broadly found in most nature systems.

Bibliography

[1] S. Gueron, S.A. Levin, D.I. Rubenstein, "The dynamics of herds: From individuals to aggregations," J Theor Biol, vol. 182, pp. 85–98, 1996.

[2] J.T. Emlen, "Flocking behaviour in birds," The Auk, vol. 69, pp. 160 –170, 1952.

[3] V. Schaller, C. Weber, C. Semmrich, E. Frey, A.R. Bausch, "Polar patterns of driven filaments," Nature, vol. 467, pp. 73–77, 2010.

[4] C. Allison, C. Hughes, "Bacterial swarming: an example of prokaryotic differentiation and multicellular behaviour," Sci. Progress, vol. 75, pp. 403–422, 1991.

[5] E.M. Rauch, M.M. Millonas, D.R. Chialvo, "Pattern formation and functionality in swarm models," Physics Letters A, vol. 207, pp. 185-193, 1995.

[6] I. Couzin, "Collective minds," Nature, vol. 445, pp. 715, 2007.

[7] C.W. Reynolds, "Flocks, Herds, and Schools: A Distributed Behavioral Model," Computer Graphics, vol. 21, pp. 25-34, 1987.

[8] P. Szabo, M. Nagy, T. VIcsek, "Transitions in a self-propelled-particles model with coupling of accelerations," Phys. Rev. E, vol. 79, pp. 021908, 2009.

[9] T. Vicsek, A. Czirok, E. Ben-Jacob, O. Shochet, "Novel Type of Phase Transition in a System of Self-Driven Particles," Phys Rev Lett, vol. 75, pp. 1226-1229, 1995.

[10] J. Buhl, D.J.T. Sumpter, I.D. Couzin, J.J. Hale, E. Despland, E. R. Miller and S. J Simpson, "From Disorder to Order in Marching Locusts," Science, vol. 312 pp. 1402, 2006.

[11] G. Gregoire, H. Chate, Y. Tu, "Moving and staying together without a leader," Physica D. vol. 181, pp. 157–170, 2003.

[12] G. Gregoire, H. Chate, Y, "Onset of collective and cohesive motion," Phys Rev Lett, vol. 92, pp. 025702, 2004.

[13] I.L. Bajec, N. Zimic, M. Mraz, "Simulating flocks on the wing: the fuzzy approach," J theor Biol, vol. 233, pp. 199-220, 2005.

[14] M. Ballerini, N. Cabibbo, R. Candelier, A. Cavagna, E. Cisbani, I.Giardina, et al, "Empirical investigation of starling flocks: a benchmark study in collective animal behaviour," Animal Behavior, vol. 76, pp. 201-215, 2008.

[15] M. Ballerini, N. Cabibbo, R. Candelier, A. Cavagna, E. Cisbani, I.Giardina, et al, "Interaction ruling animal collective behavior depends on topological rather than metric distance: Evidence from a field study," PNAS, vol.105 pp. 1232-1237, 2008.

[16] A. Cavagnaa, A. Cimarellib, I. Giardinaa, G. Parisib, R. Santagatib, F. Srefanini, et al, "Scale-free correlations in starling flocks," PNAS, vol. 107, pp. 11865-11870, 2010.

[17] Procaccini, A., et al. Propagating waves in starling, Sturnus vulgaris, flocks under predation. *Anim. Behav.* 82, 759-765 (2011).

[18] Couzin, I.D., Krause, J., James, R., Ruxton. G.D., Franks, N.R. Collective memory and spatial sorting in animal groups. *J. Theor. Biol.* 218, 1-11 (2002).

[19] Hemelrijk, C.K., et al. Emergence of oblong school shape: models and empirical data of fish. *Ethology* 116, 1099-1112 (2010).

[20] Bode, W.F., Franks, D.W., Wood, A.J. Limited Interactions in Flocks: Relating Model Simulation to Empirical Data. *J. R. Soc. Interface* 8, 301–304 (2010).

[21] Niizato, T., Gunji, Y.P. Fluctuation-driven flocking movement in three dimensions and scale-free correlation. *PLoS One* 7, e35615 (2012).

[22] Gunji, Y.P., Murakami, H., Niizato, T., Sonoda, K., Adamatzky, A. Passively Active - Actively Passive Mutual Anticipation in a Communicative Swarm. *Integral Biomathics: Tracing the Road to Reality*, Simeonov [PL et al. (ed.)] [169-180] (Springer, 2012).

[23] Katz, Y., Tunstrøm, K., Ioannou, C.C., Huepe, C., Couzin, I.D. Inferring the structure and dynamics of interactions in schooling fish. *Proc. Natl Acad. Sci. USA* 108, 18720-18725 (2011).

[24] Cavagna, A., et al. Diffusion of individual birds in starling flocks. *Proc. R. Soc. B* 280, 1471-2954 (2013).

[25] Handegard, N.O., Leblanc, S., Boswell, K., Tjostheim, D., Couzin, I.D. The dynamics of coordinated group hunting and collective information-transfer among schooling preys. *Curr. Biol.* 22, 1213-1217 (2012).

[26] Yates, C.A., Erban, R., Escudero, C., Couzin, I.D., Buhl, J., Kevrekidis, I.G., et al. Inherent noise can facilitate coherence in collective swarm motion. *Proc. Natl Acad. Sci. USA* 106, 5464-5469 (2009).

[27] Murakami, H., Tomaru, T., Nishiyama, Y., Moriyama, T., Niizato, T., et al. Emergent Runaway into an Avoidance Area in a Swarm of Soldier Crabs. *PLoS ONE* 9, e97870 (2014).

[28] Strandburg-Peshkin A, Twomey CR, Bode NMF, Kao AB, Katz Y, Ioannou CC, Rosenthal SB, Torney CJ, Wu HS, Levin SA, and ID Couziz ID (2010) Visual sensory networks and effective information transfer in animal groups. *Curr Biol* 23, 711-712.

[29] Tunstrøm K, Katz Y, Ioannou CC, Huepe C, Lutz MJ, *et al*. (2013) Collective states, multistability and transitional behavior in schooling fish. *PLoS Comput Biol*. 9 e1002915.

[30] Berdahl A, Torney CJ, Ioannou CC, Faria J. Couzin ID (2013) Emergent sensing of complex environments by mobile animal groups, *Science* 339, 574-576.

[31] Pike TW, Laland KN (2010) Conformist learning in nine-spined sticklebacks' foraging decisions. *Biol Lett* 6, 466–468.

[32] Pike TW, Kendal JR, Rendell LE, Laland KN (2010) Learning by proportional observation in a species of fish. *Behav Ecol* 21, 570–575.

[33] Reynolds CW (1987) Flocks, Herds, and Schools: A Distributed Behavioral Model. *Comput Graph* 21, 25-34.

[34] Dunlop R, Millsopp S, Laming P (2006) Avoidance learning in goldfish (Carassius auratus) and trout (Oncorhynchus mykiss) and implications for pain perception. *Appl Anim Behav Sci* 97, 255–271.

[35] Shirakawa T, Gunji YP, Miyake Y (2011) An associative learning experiment using the plasmodium of Physarum polycephalum. *Nano Commun Netw* 2, 99–105.

[36] Bradshaw C, Scoffin TP (1999) Factors limiting distribution and activity patterns of the soldier crab Dotilla myctiroides in Phuket, South Thailand. *Mar Biol* 135, 83-87.

[37] Shih JT (1995) Population-densities and annual activities of Mictyris brevidactylus (Stimpson, 1858) in the Tanshui mangrove swamp of northern Taiwan. *Zool Stud* 34, 96-105.

[38] Davie PJF, Shih HT, Chan BKK (2010) A new species of Mictyris (Decapoda, Brachyura, Mictyridae) from the Ryukyu Island, Japan. *Crustaceana Monographs* 11, 83-105.

[39] Takeda S, Murai M (2004) Microhabitat Use by the Soldier Crab Mictyris brevidactylus (Brachyura: Mictyridae): Interchangeability of Surface and Subsurface Feeding through Burrow Structure Alteration. *J Crustac Biol* 24, 327-339.

[40] Murakami H, Niizato T, Gunji YP (2012) A Model of Scale-Free Proportion Based on Mutual Anticipation. *IJALR*, 3, 35-45.

[41] Gunji YP, Nishiyama Y, Adamatzky A (2011) Robust Soldier Crab Ball Gate. *Complex systems* 20, 93-104.

[42] Gunji YP, Murakami H, Niizato T, Adamatzky A, Nishiyama Y, Enomoto K, Toda M, Moriyama T, Matsui T, Iizuka K (2011) Embodied swarming based on back propagation through time shows water-crossing, hour glass and logic-gate behavior. *Advances in Artificial Life* (Lenaerts, T. et al. eds.), 294-301

[43] Viswanathan, G.M., da Luz M.G.E., Raposo, E.P. and Stanley, H.E.(2011) The Physics of Foraging: An Introduction to Random Searches and Biological Encounters, Cambridge University Press, Cambridge

[44] Viswanathan, G.M., Raposo, E.P. and da Luz M.G.E. (2008) Lévy flights and superdiffusion in random search: the biological encounters context, *Phys. Life Rev.* 5:133–162.

[45] Reynolds, A.M. and Rhodes, C.J. (2009) The Lévy flight paradigm: random search patterns and mechanisms. *Ecology*. 90(4):877-887.

[46] Humphries, N.E., Queiroz, N., Dyer, J.R.M., Pade, N.G., Musyl, M.K., Schaefer, K.M., Fuller, D.W. Brunnschweiler, J.M., Doyle, T.K., Houghton, J.D.R., Hays, G.C., Jones, C.S., Noble, L.R., Wearmouth, V.J. Southall, E.J. and Sims, D.W. (2010) Environmental context explains Lévy and Brownian movement patterns of marine predators. *Nature.* 465:1066–1069.

[47] Cole, B.J. (1995) Fractal time in animal behavior: The movement activity of Drosophila. *Anim Behav*. 50:1317–1324.

[48] Viswanathan, G.M., Afanasyev, V., Buldyrev, S.V., Murphy, E.J., Prince, P.A. and Stanley, H.E. (1996) Lévy flight search patterns of wandering albatrosses, Nature 381:413–415.

[49] Edwards AM, et al. (2007) Revisiting Lévy flight search patterns of wandering albatrosses, bumblebees and deer. Nature 449(7165):1044–1048.

[50] Humphries, N.E., Weimerskirch, H., Queiroz, N., Southall, E.J. and Sims, D.W. (2012) Foraging success of biological Lévy flights recorded in situ. *PNAS*. 109(19):7169-7174.

[51] O'Brien, W.J., Browman, H.I. and Evans, B.I. (1990) Search strategies of foraging animals. *Am Sci* 78:152–160.

[52] Bénichou, O., Loverdo, C., Moreau, M. and Voituriez, R. (2011) Intermittent search strategies. *Rev. Modern Phys*. 83: 81–129.

[53] March, J.G., (1991) Exploration and exploitation in organizational learning. *Organization Science*. 2:71–87.

[54] Kareiva, P.M., Shigesada, N. (1983) Analyzing insect movement as a correlated random walk. *Oecologia.* 56:234–238.

[55] Bartumeus, F. and Levin, S.A. (2008) Fractal reorientation clocks: Linking animal behavior to statistical patterns of search. *PNAS*. 105(49): 19072–19077.

[56] Santos, M.C., Boyer, D., Miramontes, O., Viswanathan, G.M., Raposo, E.P., Mateos, J.L. and da Luz, M.G.E. (2007) The origin of power-law distributions in deterministic walks: the influence of landscape geometry, *Phys. Rev. E*. 75:061114-061120.

[57] Benhamou, S. (2007) How many animals really do the Lévy walk? *Ecology.* 88(8): 1962–1969.

[58] Cavagnaa A., et al.: Information transfer and behavioural inertia in starling flocks. *Nature physics.* 10, 691/696 (2014).

[59] Tanaka, Y., Iguchi, K., Yoshimura, J., Nakagiri, N., Tainaka, K. Historical effect in the territoriality of ayu fish. *J. Theor. Biol.* 268, 98-104 (2011).

[60] Viswanathan, G.M., Raposo, E.P., Bartumeus, F., Catalan, J., da Luz, M.G.E. Necessary criterion for distinguishing true superdiffusion from correlated random walk processes. *Phys. Rev. E* 72, 1 – 6 (2005).

[61] Cattuto, C., Van den Broeck, W., Barrat, A., Colizza, V., Pinton, J-F., et al. Dynamics of Person-to-Person Interactions from Distributed RFID Sensor Networks. *PLoS ONE* 5, e11596 (2010).

[62] Stehlé, J., Voirin, N., Barrat, A., Cattuto, C., Isella, L., et al. High-Resolution Measurements of Face-to-Face Contact Patterns in a Primary School. *PLoS ONE* 6, e23176 (2011).

[63] Starnini, M., Baronchelli, A., Pastor-Satorras, R. Modeling Human Dynamics of Face-to-Face Interaction Networks. *Phys. Rev. Lett.* 110, 168701 (2013).

[64] Reynolds, A.M., Frye, M.A. Free-Flight Odor Tracking in Drosophila Is Consistent with an Optimal Intermittent Scale-Free Search. *PLoS ONE* 2, e354 (2007).

[65] Bazazi, S., Bartumeus, F., Hale, J.J., Couzin, I.D. Intermittent Motion in Desert Locusts: Behavioral Complexity in Simple Environments. *PLoS Comput Biol* 8, e1002498 (2012).

[66] Tu, Y., Toner, J., Ulm, M. Sound waves and the absence of Galilean invariance in flocks. *Phys. Rev. Lett.* 80, 4819 – 4822 (1998).

[67] Takeda S (2005) Sexual differences in behavior during the breeding season in the soldier crab (Mictyris brevidactylus). *J Zool Lond* 266, 197-204.

[68] Helbing D, Schweitzer F, Keltsch J, Molnár P (1997) Active walker model for theformation of human and animal trail systems. *Phys Rev E* 56, 2527-2539.

[69] Goldstone RL, Gurechis TM (2009) Collective Behavior. *Topics in cognitive science* 1, 412-438.

[70] Kunz H, Hemelrijk CK (2003) Artificial fish schools: collective effects of school size, body size, and body form, *Artificial life* 9: 237-253.

[71] Romanczuk P, Couzin ID, Schimansky-Geier L (2009) Collective motion due to individual escape and pursuit response. *Phy Rev Let* 102, 010602.

[72] Bartumeus F., da Luz M.G.E., Viswanathan G.M. and Catalan J. (2005) Animal search strategies: a quantitative random walk analysis. *Ecology*. 86(11): 3078-3087.

[73] Gunji, Y.P., Shirakawa, T., Niizato, T., Yamachiyo, M. and Tani, I. (2011) An adaptive and robust biological network based on the vacant-particle transportation model. *J Theor Biol.* 272:187-200.

[74] Ferreira, A.S., Raposo, E.P., Viswanathan, G.M. and da Luz M.G.E. (2012) The influence of the environment on Lévy random search efficiency: Fractality and memory effects, *Physica A*. 391:3234-3246.

[75] MacNamara, J.M., Houston, A.I. (1987) Memory and the efficient use of information, *J. Theoret. Biol.* 125:385–395.

[76] Niizato T., et al: Emergence of the scale-invariant proportion in a flock from the metric-topological interaction. *Biosystems* 119, 62/68. (2014)

[77] MacArthur RH, Pianka ER. 1966. On optimal use of a patchy environment. Am Nat 100: 603–609.

[78] López- López P, Benavent-Corai L, García-Ripollés C, Urios V. 2013. Scavengers on the move: behavioural changes in foraging search patterns during the annual cycle. PLoS ONE 8: e54352.

[79] Cox DR. 1955. Some Statistical Methods Connected with Series of Events. Journal of the Royal Statistical Society Series B-Statistical Methodology 17: 129–164.